

**BEHAVIOUR OF ECCENTRICALLY LOADED CIRCULAR
FOOTING ON GRANULAR SOIL**

*RESEARCH PROJECT SUBMITTED IN PARTIAL FULFILLMENT OF
REQUIREDMENTS FOR THE DEGREE OF*

**MASTER OF TECHNOLOGY IN
(GEOTECHNICAL ENGINEERING)**

SUBMITTED BY

SARITA JENA

ROLL NO-213CE1044

UNDER THE GUIDANCE OF

PROF.C.R PATRA



**DEPARTMENT OF CIVIL ENGINEERING NATIONAL
INSTITUTE OF TECHNOLOGY ROURKELA, 2015**



CERTIFICATE

This is to certify that the thesis entitled as “*Behaviour of eccentrically loaded circular footing on granular soil*” is a record of bonafide work and sincere efforts put forward by Sarita jena submitted for the requirement of the degree of **Master of Technology in Civil Engineering** with specialization in **Geotechnical engineering** at National Institute of Technology Rourkela, under my supervision and Guidance. To the best of my knowledge, the content in this report has not been submitted to any other university/institute for the award of any degree or diploma.

Prof. Chittaranjan Patra
Department of Civil Engineering
National Institute of Technology
Rourkela

ACKNOWLEDGEMENT

I would like to express my deep sense of gratitude to my esteemed supervisor **Prof. Chittaranjan Patra**, for his encouragement and consistent support throughout the research work in the last one year. I would genuinely acknowledge his faith in me, to do this work, taking it to a higher level.

I would like to extend my sincere thanks to **Prof. S.K. Sahu, HOD, Civil Engineering Department**, National Institute of Technology, Rourkela, who have illuminated me throughout my research work with his enormous support.

I am also honored, for **Prof. N. Roy, Prof. S.K. Das, Prof. S.P. Singh, Prof. R.K. Bag, Prof. S. Patra, Prof. R.N. Behera** and all other faculty members of Civil Engineering Department, NIT Rourkela, having their valuable support during my research work.

Exceptional and sincere thanks to **Miss. Roma Sahu**, and **Mr. Barada Prasad Sethy** Ph.D. Scholars in Civil Engineering Department, NIT Rourkela for their suggestions, remarks, emotional and consistent support during the crucial period of research work.

I am also appreciative to Mr. A. K Nanda, Technical Assistant, Geotechnical Engineering Laboratory, NIT Rourkela for his remarkable support during my research work.

I am also thankful to Mr. Chamuru Suniani (Geotechnical Lab Attendant), Mr. Harihar Garnayak (Highway Lab Attendant), Mr. Suraj and Mr. Saroj for their support & co-operation throughout the project work.

At long last, I would thank my family members for their unconditional moral support, a special thanks to my father, for being there for me, sailing my boat through all hardships.

Sarita Jena

Roll No-213CE1044

ABSTRACT

In the past several works have been carried out for eccentric loaded condition over sand for finding the ultimate bearing capacity of shallow foundation. These investigations are limited to strip, square and rectangular footings, it has been found out that less attention is paid to determine the ultimate bearing capacity of eccentrically loaded circular foundation with different depth of embedment D_f . Hence the present investigations are based on the load settlement behaviour of eccentrically loaded circular footing. Bearing capacity is different for centric and eccentric vertical loaded condition which is subjected to the foundation, the case of vertical load applied centrally to the foundation studied in most of the cases. Settlement and bearing capacity study of shallow footings is needed for design of a foundation. The investigation is undertaken to study the behaviour of bearing capacity and settlement of circular footing over sand bed. The test have been conducted for both surface and embedded foundations under eccentric and centric loads resting over sand bed. The investigation shows that ultimate bearing capacity of foundation depends on the different type of loading (Centric, eccentric) and the depth of embedment (D_f/B). Tests were carried out at depth of embedment (D_f/B) varies from zero to one and the eccentricity ratio (e/B) varies from zero to 0.15 with sand of relative density (D_r) equal to 69%. The present experiment is also analyzed and compared with the results of the previous investigations. In order to predict load-settlement behaviour and compare with experimental observation, equally analytical and numerical analysis (PLAXIS 3D) have also been conducted.

CONTENTS

| Title | Page No. |
|------------------------------------------------------------------|----------|
| Abstract..... | iii |
| Table of contents..... | ix |
| List of tables..... | viii |
| List of figures..... | vi |
| List of Notations..... | ix |
| CHAPTER1: INTRODUCTION..... | 1 |
| 1. Introduction..... | 2 |
| CHAPTER2: LITERATURE REVIEW..... | 4 |
| 2.1 introduction..... | 5 |
| 2.2 Bearing capacity of shallow foundation on granular soil..... | 5 |
| CHAPTER3: MATERIAL USED AND EXPERIMENTAL PROCEDURE..... | 17 |
| 3.1 Introduction..... | 18 |
| 3.2 Material used..... | 18 |
| 3.2.1 Sand..... | 18 |
| 3.2.2 Characteristics of sand..... | 19 |
| 3.3 Experimental procedure..... | 19 |
| 3.4 Model test series..... | 22 |
| CHAPTER 4: RESULTS AND ANALYSIS..... | 23 |
| 4.1 Introduction..... | 24 |
| 4.2 Centric loading condition..... | 24 |
| 4.2.1 Surface footing with centric loading condition..... | 25 |
| 4.2.2 Embedded footing with centric loading condition..... | 26 |
| 4.3 Eccentric loading condition..... | 31 |

| | |
|--------------------------------------------------------------|----|
| 4.3.1 Surface footing with eccentric loading condition..... | 31 |
| 4.3.2 Embedded footing with eccentric loading condition..... | 33 |
| CHAPTER 5: SUMMERY OF RESULTS | 43 |
| 5.1 Conclusion..... | 44 |
| CHAPTER 6: NUMERICAL ANALYSIS..... | 45 |
| 6.1 Introduction..... | 46 |
| 6.2Methodology..... | 47 |
| 6.2.1 Testing procedure..... | 48 |
| 6.3 Results analysis..... | 50 |
| 6.3.1 Comparison..... | 54 |
| CHAPTER 7: CONCLUSION AND SCOPE OF FUTURE RESEARCH WORK..... | 59 |
| 7.1 Conclusion..... | 60 |
| 7.2 Future research work..... | 61 |
| CHAPTER 8: REFERENCES..... | 62 |

LIST OF FIGURES

| Figure no. | Title | Page no. |
|--------------|----------------------------------------------------------------------------------------------------------------------------------------------|----------|
| Figure 1 | Typical failure mechanism of axially loaded footing | 3 |
| Figure 2 | Effective width concept (source: Meyerhof, 1953) | 7 |
| Figure 2.1 | Geometry of the finite element mesh and details of the mesh in the near field | 12 |
| Figure 3.1 | Grain size distribution of soil | 20 |
| Figure 3.2 | Experimental setup of laboratory model tests at Surface condition | 21 |
| Figure 3.3 | Experimental setup of laboratory model tests at embedded condition | 22 |
| Figure 4.1 | Ultimate Bearing Capacity q_u by Tangent Intersection method | 25 |
| Figure 4.2 | Load Settlement curve with $D_f/B=0$, $e/B=0$ | 26 |
| Figure 4.3 | Variation of Load-Settlement Curve with Embedment ratio (D_f/B) at $e/B=0$ | 27 |
| Figure 4.4 | Variation of q_u with D_f/B for $e/B = 0$ using formulae of existing theories along with present experimental values | 28 |
| Figure 4.5 | Change of N with B (adapted after DeBeer, 1965) | 29 |
| Figure 4.6 | Comparison between N obtained from tests with small footings and large footings of 1m^2 area on sand (adapted after DeBeer, 1965) | 30 |
| Figure 4.7 | Load Settlement Curve with $D_f/B=0$, $e=0, 0.05B, 0.10B, 0.15B$ | 33 |
| Figure 4.8 | Load-Settlement Curve with $D_f/B=0.5$, $e=0, 0.05B, 0.10B, 0.15B$ | 34 |
| Figure 4.9 | Load-Settlement Curve with $D_f/B=1$ $e=0, 0.05B, 0.10B, 0.15B$ | 35 |
| Figure 4.10 | Difference in Load-Settlement Curve with Embedment ratio (D_f/B) at $e/B=0.05$ | 35 |
| Figure 4.11 | Difference in Load-Settlement Curve with Embedment ratio (D_f/B) at $e/B=0.10$ | 36 |
| Figure 4.12: | Difference in Load-Settlement Curve with Embedment ratio (D_f/B) at $e/B=0.15$ | 36 |
| Figure 4.13 | Comparison of ultimate bearing capacities of Present experimental results With Meyerhof at different D_f/B and e/B | 38 |
| Figure 4.14 | Comparison of Present experimental results with Purkayastha and Char (1977) with $D_f/B=0$ | 40 |
| Figure 4.15 | Comparison of Present experimental results with Purkayastha and Char (1977) with $D_f/B=0.5$ | 40 |

| | |
|-------------------------------------------------------------------------------------------------------------------------------------------------------|----|
| Figure 4.16 Comparison of Present experimental results with Purkayastha and Char (1977) With $D_f/B=1.0$ | 41 |
| Figure 6.1 General procedure of analysis | 48 |
| Figure 6.2 Geometry model for analysis in surface condition | 49 |
| Figure 6.3 Geometry model for analysis in surface eccentric condition | 49 |
| Figure 6.4 Failure pattern at eccentric condition ($e/B=0.15$) | 50 |
| Fig.6.5 q_u value shown by tangent intersection method at $e/B=0$, $D_f/B=0$ | 51 |
| Figure 6.6 Variation in Load settlement curve at $D_f/B=0$ | 52 |
| Figure.6.7 Variation in Load settlement curve at $D_f/B=0.5$ | 53 |
| Figure 6.8 Variation in Load settlement curve at $D_f/B=1$ | 53 |
| Figure 6.9 Comparison Load settlement curve at $D_f/B=0$, $e/B=0$ | 54 |
| Figure 6.10 Comparison Load settlement curve at $D_f/B=0$, $e/B=0.05$ | 54 |
| Figure 6.11 Comparison Load settlement curve at $D_f/B=0$, $e/B=0.10$ | 56 |
| Figure 6.12 Comparison Load settlement curve at $D_f/B=0$, $e/B=0.15$ | 56 |
| Figure 6.13 Comparison of ultimate Bearing capacity at different e/B (0, 0.05, 0.10, and 0.15) for present experiment results with PLAXIS result | 58 |

LIST OF TABLES

| Table no. | Title | Page no. |
|-----------|-----------------------------------------------------------------------------------------------------------------------------------|----------|
| Table 2 | Summary of bearing capacity factors | 9 |
| Table 2.1 | Summary of shape and Depth factors | 10 |
| Table 2.2 | Value of a and k | 11 |
| Table 3.1 | Geotechnical property of sand | 19 |
| Table 3.2 | Sequence of the model test series | 22 |
| Table 4.1 | Model test parameters for the case of Centric Loading condition | 24 |
| Table 4.2 | Calculated values of ultimate bearing capacities q_u by different theories along with Present experiment value | 31 |
| Table 4.3 | Model test parameters for the case of Eccentric Loading condition | 32 |
| Table 4.4 | Calculated values of (q_u) by Meyerhof (1963) for eccentric condition along with Present experimental values of q_u | 39 |
| Table 4.5 | Calculated values of R_k by Purkayastha and Char (1977) for eccentric vertical condition along with Present experimental values | 42 |
| Table 6.1 | Parameter used in numerical analysis | 47 |
| Table 6.2 | Calculated value of q_u by PLAXIS for eccentric condition along with experimental value | 57 |

LIST OF NOTATION

List of Abbreviations and Nomenclature

Abbreviations

| | |
|-----|---------------------------|
| RF | Reduction factor |
| UBC | ultimate bearing capacity |

Nomenclature

Symbols

| | |
|----------------------|----------------------------------------------------|
| B | Width of foundation (Diameter of circular footing) |
| t | Thickness of foundation |
| L | Length of foundation |
| e | Load eccentricity |
| Q_U | Ultimate load per unit length of foundation |
| q_u | Ultimate load bearing capacity |
| D_f | Depth of foundation |
| γ | Unit weight of sand |
| $\gamma_{d(\max)}$ | Maximum dry unit weight of sand |
| $\gamma_{d(\min)}$ | Minimum dry unit weight of sand |
| q | Surface surcharge |
| N_c, N_q, N_γ | Bearing capacity factors |
| S_c, S_q, S_γ | Shape factors |
| d_c, d_q, d_γ | Depth factors |
| ϕ | Internal angle of friction |
| δ | Dilatancy angle |

| | |
|----------|-------------------------------|
| c | Cohesion |
| C_u | Uniformity coefficient |
| C_c | Coefficient of curvature |
| S | Settlement |
| S_u | Ultimate settlement |
| A' | Effective area of foundation |
| B' | Effective width of foundation |
| G | Specific gravity |
| D_{10} | Effective particle size |
| D_{30} | Particle size |
| D_{60} | Particle size |
| D_r | Relative density |

CHAPTER 1

INTRODUCTION

1.1 Introduction

The lowest part of a structure which transfers its load to the soil beneath is known as foundation. The stability of a structure mostly depends on the performance of foundation. Its design should be done properly, considering its importance. Depending on the depth of embedment, foundations can be classified as shallow or deep. The ultimate load which can be sustained by the soil is identified as bearing capacity. Bearing capacity and settlement are two parameter requirement for the design of shallow foundation. It is essential for engineers to estimate the foundation's bearing capacity subjected to vertical loads. Usually, so many studies for estimation of bearing capacity involves foundation subjected to vertical loading. However, for some structures such as abutment, retaining wall, portal framed building and water front structure, which are often subjected to eccentric load due to horizontal thrust and bending moment. Settlement of foundation under load due to the movement of soil particle horizontally and vertically below the footing. Tilt of the footing caused by eccentric loading which results to non-uniform stress distribution and unequal settlement below the footing. When centric vertical load subjected to the foundation, uniform stress distribution under the footing and equal settlement at both edges occurred. The tilt of footing directly proportional to the (e/B) ratio, i.e. it increases with the increasing (e/B) ratio. When eccentricity ratio is greater than $1/6$, the edge of the footing which is away from center will lose its contact with the soil. As a result, it will reduce the effective width (B') of footing and which will reduce the ultimate bearing capacity of foundation. Stress developed in different layers of soil due to the imposed load by various structures at the foundation level will always be accompanied by some amount of strain, which causes settlement of the structures.

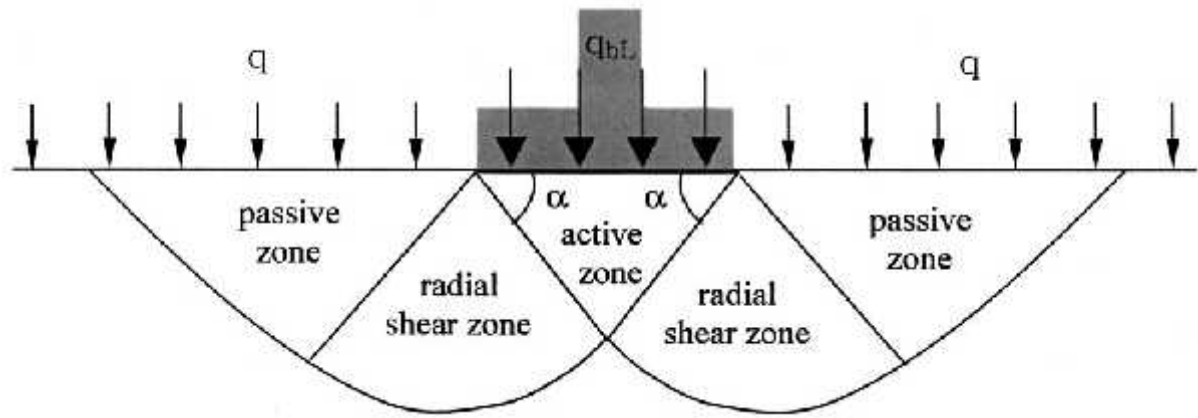


(Figure 1: Typical Failure Mechanism of Axially Loaded Footing)

CHAPTER 2

LITERATURE REVIEW

2.1 Introduction

The review of literatures briefly represented below for eccentrically loaded foundation. An overview of experimental study and numerical analysis is also discussed below.

2.2 Bearing Capacity of Shallow Foundations on granular soil

For stability the foundation of structure should be stable against shear failure of the supporting soil and to avoid damage to the structure it must not settle beyond a tolerable limit. The stability of the supporting soil to the foundation of structure shows the stability to structure. A foundation should not exceed its ultimate bearing capacity for performing to its optimum capacity. After the publications of Terzaghi (1943) concept on the field of bearing capacity for shallow foundations, numerous studies have been made by various investigators. Several studies are related to footings subjected to vertical and central loads. Researchers like Purkayastha and char (1977) and Prakash and saran (1971) studied on the eccentrically loaded footings. Empirical procedures for estimating the ultimate bearing capacity of foundations subjected to eccentric vertical loads developed by Meyerhof (1953). Meyerhof (1974) modified the shape factor and depth factor for bearing capacity analysis in circular footing over rigid sand bed. An extensive literature review based on bearing capacity of shallow foundations under eccentric loading conditions is presented below.

Terzaghi (1943) theory was proposed first to determine the ultimate bearing capacity of Shallow footing. The surcharge $q = D$ applied on soil above the bottom of foundation. The study of foundation as strip foundation with rough base. As per this theory shallow foundation having the depth less than or equal to width. The zone of failure below the foundation is divided in to 3 part i.e. Triangular zone, 2 Radial shear zone, and 2 Rankine passive zone due to vertical centric load. He had provided expression for the different type of footing as below

$$q_u = cN_c + qN_q + \frac{1}{2}\gamma BN_\gamma \quad \text{For continuous and strip foundation}$$

$$q_u = 1.3cN_c + qN_q + 0.4\gamma BN_\gamma \quad \text{For square foundation}$$

$$q_u = 1.3cN_c + qN_q + 0.3\gamma BN_\gamma \quad \text{For Circular foundation}$$

Where c =Cohesion of soil, γ = Unit weight of soil and $q = \gamma D_f$, N_c, N_q , and N_γ are the bearing capacity factors are given below

$$N_c = \cot \phi' \left[\frac{e^{2\left(\frac{3f}{4} - \frac{\phi'}{2}\right) \tan \phi'}{2 \cos^2\left(\frac{f}{4} + \frac{\phi'}{2}\right)} - 1 \right]$$

$$N_q = \left[\frac{e^{2\left(\frac{3f}{4} - \frac{\phi'}{2}\right) \tan \phi'}}{2 \cos^2\left(45 + \frac{\phi'}{2}\right)} \right]$$

$$N_\gamma = \frac{1}{2} \left(\frac{K_p \gamma}{\cos^2 \phi'} - 1 \right) \tan \phi'$$

Where K_p = passive pressure coefficient

Meyerhof (1953) proposed a generalized equation for any shape of foundation (strip, rectangular or square) in case of ultimate bearing capacity since the case of rectangular footing was not reported by Terzaghi (1943). The proposed equation for ultimate bearing capacity is as follows

$$B' = B - 2e$$

where e = load eccentricity

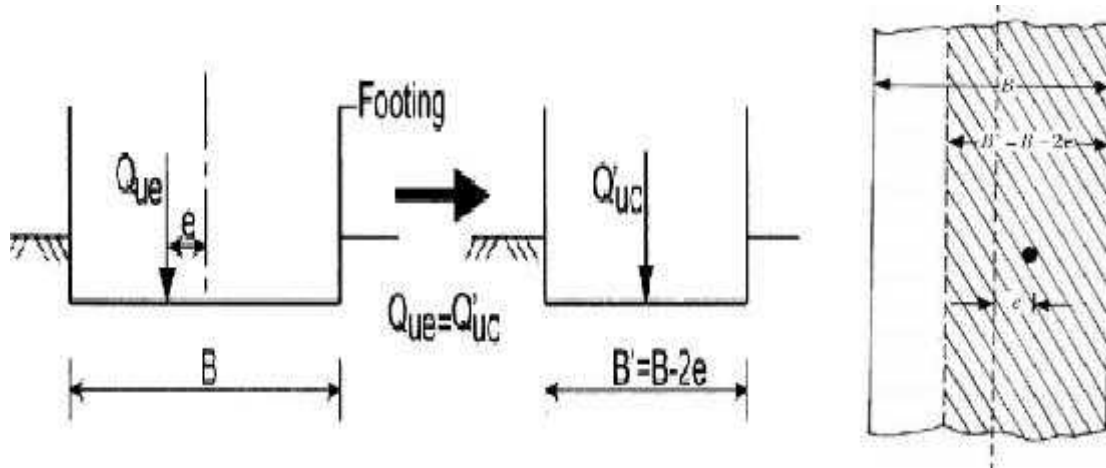


Figure 2: Effective width concept (source: Meyerhof, 1953)

$$Q_{ult} = q_u (A')$$

Where A' = effective area = $B' \times 1$ He concluded that the average bearing capacity of the footing decreases, approximately parabolic ally, with an increase in eccentricity.

Meyerhof (1963) suggested a bearing capacity equation in generalized form for different shape of footing and also the study not considered the shearing resistance across the failure surface in soil above the bottom of foundation. Below equation is given for ultimate bearing capacity.

$$q_u = cN_c F_{cs} F_{cd} F_{ci} + qN_q F_{qs} F_{qd} F_{qi} + \frac{1}{2} \gamma B N_\gamma F_{\gamma s} F_{\gamma d} F_{\gamma i}$$

$$F_{cs}, F_{qs}, F_{\gamma s} = \text{Shape factor,}$$

$$F_{cd}, F_{qd}, F_{\gamma d} = \text{Depth factor}$$

$$F_{ci}, F_{qi}, F_{\gamma i} = \text{Inclination factor}$$

In the past many investigators have proposed bearing capacity factors. These factors are summarized in table

Table 2: Summary of bearing capacity factors

| Bearing capacity factors | Equation | Investigator |
|--------------------------|-------------------------------------------------------------------------------------------------------------------------------------|----------------------------------------------------------------------------|
| N_c | $N_c = (N_q - 1) \cot \phi$ | Terzaghi (1943), Meyerhof (1963) |
| N_q | $N_q = \left[\frac{2 \left(\frac{3f}{4} - \frac{w'}{2} \right) \tan \phi'}{2 \cos^2 \left(45 + \frac{\phi'}{2} \right)} \right]$ | Terzaghi (1943) |
| N_q | $N_q = \tan^2 \left(45 + \frac{\phi}{2} \right) e^{(f \tan \phi)}$ | Meyerhof(1963), Hansen(1970), Vesic(1973), Is code(IS: 6403-1981) |
| N_γ | $N_\gamma = 1.8(N_q - 1) \cot \phi (\tan \phi)^2$ | Terzaghi (1943) |
| N_γ | $N_\gamma = 1.5(N_q - 1) \tan \phi$ | Hansen(1970) |
| N_γ | $N_\gamma = 2(N_q + 1) \tan \phi$ | Vesic(1973) Is code(IS: 6403-1981) |

Table 2.1: Summary of shape and Depth factors

| Factors | Equation | Investigator |
|---------|----------------------------------------------------------------------------------------------------------------------------------------------------------------------------------------|------------------------------|
| Shape | $S_q = 1$ $S_x = 0.6$ (circular footing) | Meyerhof (1974) |
| | $S_q = 1 + \left(\frac{B}{L}\right) \tan \omega$ $S_x = 1 - 0.4 \left(\frac{B}{L}\right)$ | Vesic (1975) Hansen(1970) |
| | $S_q = 1$ $S_x = 0.6$ (circular footing) | Is code (IS: 6403-1981) |
| Depth | $w \geq 10^\circ : d_c = 1 + 0.2 \left(\frac{D_f}{B}\right) \tan \left(45 + \frac{w}{2}\right)$ $d_q = d_x = 1 + 0.1 \left(\frac{D_f}{B}\right) \tan \left(45 + \frac{w}{2}\right)$ | Meyerhof(1963) |
| | $For \frac{D_f}{B} \leq 1 : d_c = d_q - \frac{1 - d_q}{N_q \tan \omega} (For \omega > 0)$ $d_q = 1 + 2 \tan \omega (1 - \sin \omega)^2 \left(\frac{D_f}{B}\right)$ $d_x = 1$ | Hansen(1970) Vesic(1975) |
| | $d_q = d_x = 1 + 0.1 \left(\frac{D_f}{B}\right) \sqrt{\tan^2 \left(45 + \frac{w}{2}\right)} (For \omega > 10^\circ)$ | Is code (IS: 6403-1981) |

Prakash and Saran (1971) developed a relationship given to calculate the ultimate load per unit length (Q_u) of strip foundation with eccentrically vertical loaded condition shown by the following equation

$$q_u = \frac{Q_u}{(B \times 1)} = \frac{1}{2} \gamma B N_{\gamma}(e) + \gamma D_f N_q(e) + c N_c(e)$$

Where $N_{\gamma}(e)$, $N_q(e)$, $N_c(e)$ = Bearing capacity factors of continuous foundation in an eccentrically loaded condition.

Meyerhof (1974) the study was based on the ultimate bearing capacity of circular and strip footing resting on sub-soils having two layers of different cases of dense sand on soft clay and loose sand on stiff clay. Bearing capacity ratio of clay to sand, friction angle, shape and depth of foundation are the main factors which have an influence over sand layer thickness below the footing. For circular footing upper limits of $S_{\gamma} = 0.6$ and $S_q = 1$.

Purkayastha and char (1977) tests were conducted for analysis on stability of eccentrically loaded strip foundation on sand using the method of slices proposed by Janbu (1957). Based on this study

$$\frac{q_{u(e)}}{q_{u(e=0)}} = 1 - R_K$$

$$R_K = 1 - \frac{q_{u(eccentric)}}{q_{u(centric)}}$$

$$R_K = a \left(\frac{e}{B} \right)^K$$

k and a value presented in below table

Table2.2: Value of a and k

| D_f/B | a | K |
|---------|-------|-------|
| 0.00 | 1.862 | 0.73 |
| 0.25 | 1.811 | 0.785 |
| 0.50 | 1.754 | 0.80 |
| 1.00 | 1.820 | 0.888 |

Rahaman (1981) study was carried out for understanding the problem of the bearing capacity and settlement by using Circular footing on sand bed. Shear strength, Frictional angle, relative density (D_r) of sand, and surcharge effect on bearing capacity and settlement are investigated. Maximum vertical strain occurs at 0.5 to 0.6 times the diameter of footing, depth increase with decrease in density of sand. Radial deformation increase from center of the footing to a maximum value at a distance of 0.75 time the diameter and then started decreasing.

Taiebat and Carter (2002) this paper described Finite element modeling of the problem of the bearing capacity of strip and circular footings under vertical load and moment. The footings rest on the uniform and homogeneous soil surface which undergoes deformation under undrained condition. The soil has a uniform undrained Young's modulus and a uniform undrained shear strength (S_u), $E_u = 300S_u$. A Poisson's ratio of $\mu=0.5$. The Young's modulus for the foundations was set as $E_f=1000E_u$ that is, the foundations are much stiffer than the soil, and therefore they can be considered as effectively rigid. The contact between the footings and the soil is unable to sustain tension.

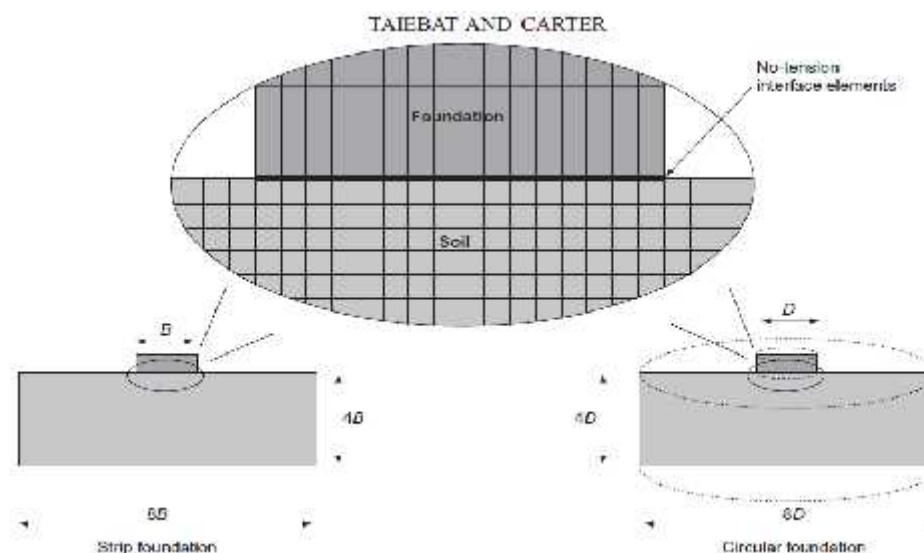


Figure 2.1: Geometry of the finite element mesh and details of the mesh in the near field

(Source: Taiebat and Carter, 2002)

To model the interface as shown in the above figure 2.1 a thin layer of ‘no-tension’ elements was used under the footing. The separation between the foundation and the soil is shown by the presence of tensile vertical stress in the interface elements. No shear stress can be sustained in the interface elements immediately after the separation. However, comparison of the failure envelopes obtained in the study shows that the effective width method, generally used in the analysis of footing which is subjected to eccentric load and it provide approximate values of the collapse loads.

Boushehrian and Hataf (2003) study was performed on circular and ring footing. Here, the effects of vertical spacing, number of reinforcement layers on bearing capacity of footing and the depth of first layer of reinforcement were considered for investigation. Both the experimental and numerical studies showed that, with the use of a single layer of reinforcement, there is an optimum reinforcement embedment depth for which the bearing capacity is greatest. They also found out that, for multi-layer reinforced sand, it requires an optimum vertical spacing of reinforcing layer. It was also found that, with the increase in number of reinforcement layers, the bearing capacity also increased, provided the reinforcements were placed within a range of effective depths. Further, the

analysis indicated that, bearing capacity does not increase beyond a threshold value of reinforcement stiffness.

Dash et al. (2003) by conducting small-scale model tests, the effectiveness of geocell reinforcement placed in the granular fill overlying soft clay beds has been studied. The test beds were applied with uniform loading by a rigid circular footing. The overall performance of the system depends on the factors such as width and height of geocell mattress and presence of a planar geogrid layer at the base of geocell mattress. The performance of the system can be improved substantially by providing geocell reinforcement in the sand layer lying above. With the addition of another geogrid layer at the base of the geocell mattress, load carrying capacity and stiffness of foundation bed increases considerably. With increase in the height of geocell mattress, this beneficial effect decreases.

Sitharam and Sireesh (2004) this paper contains the model test conducted to determine the bearing capacity of an embedded circular footing supported by multi-layer geogrid sand beds. Besides load settlement data, strain in geogrid layer, pressure distribution on soil subgrade and deformations on fill surface were measured. The results obtained from test shows that, the ultimate bearing capacity increases with embedment depth ratio of the foundation. A considerable improvement in performance in terms of increase in bearing capacity and reduction in surface deformation can be obtained by providing multi-layer geogrid reinforcement in the sand bed. It also causes uniform redistribution of footing pressure over a wide area of subgrade soil.

Cerato and Lutenecker (2006) investigation carried out on model circular and square footing test performed on well-graded sand with 3 different relative density and 5 different sand layer thickness. The foundation will have an influence over the unit load supported by the soil of the hard layer present at a certain depth. Therefore original equation of bearing capacity modified for this condition. Footing shape factor S_x should account for both shape and final layering. To predict bearing capacity on finite layer first appropriate shape factor (Square $S_x=0.8$, Circular $S_x=0.6$) should be chosen.

Basudhar et al. (2007) investigated on the Effect of the footing size, number of reinforcing layers, reinforcement placement pattern and bond length and the relative density of the soil on the load-settlement characteristics of the circular footing over sand bed with geotextile. By the increase in number of reinforcement layers settlement value decreases. There is substantially increment of BCR values for each increment in the number of reinforcement layers.

Sireesh et al. (2009) the paper based on various parameters such as, thickness of unreinforced sand layer above clay bed, width and height of geocell mattress, influence of an additional layer of planar geogrid placed at the base of the geocell mattress, relative density of the sand fill in the geocell varies in the model test. The test results shows that, by providing adequate size of geocell over the clay performance can be improved. If the height of geocell mattress is greater than 1.8 times the diameter of footing, effect of voids over the performance of footing reduces. With geocells filled with dense soil better improvement in performance can be achieved.

Lovisa et al. (2010) paper studied for circular footing to find out the behaviour of prestressed geotextile-reinforced over sand bed. A significant improvement to the load bearing capacity and settlement can be achieved by addition of prestress reinforcement. The load-carrying capacity at 5 mm settlement in the prestressed case (with prestress equal to 2% of the allowable tensile strength

of the geotextile) is approximately double that of the geotextile reinforced sand without prestress for surface footing.

Nagaraj and Ullagaddi (2010) in this paper investigation carried out to study the effect of shape and size of footing on load settlement behavior of sand foundation. In case of sand foundation the increase in size of footing will improve the bearing capacity or load – settlement behavior of the supporting soil and also the shape of the footing has influence on the bearing capacity or load - settlement behavior of the supporting soil. Square footing has shown better load-settlement behavior as compared to circular and rectangular shapes.

Dewaikar et al. (2011) observed on the model circular footing with reinforced soil to study the load settlement behaviour. The study showed that provision of a single layer reinforcement, ultimate bearing capacity increases and settlement decreases. Further, in case of BCR and SRF rubber grid performed better than the Geo-grid.

Elsaied et al. (2014) three dimensional physical laboratory models were examined to investigate the influence of soil confinement on circular footing behavior resting on granular soil. Observed that on increasing the number of geogrid layers more than one layer had a small significant effect on the footing behavior. Moreover, placing geogrid layers underneath the cylinders improves the bearing capacity up to 7.5 times that of the non-confined case. The load-settlement behavior depends on the diameter and height of the confinement cylinder relative to the footing diameter.

Gupta et al. (2014) investigation has been done on the influence of three dimensional confinement of dense sand on the behavior of a model circular footing resting over dense sand. The load bearing capacity was studied for a circular footing supported on a three-dimensional confined sand bed. The results indicate that, by confining soil the bearing capacity of circular footing can be increased

appreciably. As compared to the unconfined case the bearing capacity was found to increase by a factor of 36.18.

2.3 Scope of the present study

Based on the existing literature review for the bearing capacity of shallow foundations, it shows that very few attentions has been paid to determine the ultimate Bearing capacity of eccentrically loaded circular footing. Most of these studies are based on theoretical analyses and numerical analyses supported by few number of model tests. So, the objective of the present thesis is to study the behaviour of eccentrically loaded circular footing by varying eccentricity ratio (e/B), depth of embedment ratio (D_f/B) at 69% relative density (I_D). The experimental values have been compared with different theory of analysis. Study of Variation in Reduction factor (R_k) has been occurred for purkayastha and char (1977) and eccentrically loaded circular footings. Numerical analysis is conducted by using PLAXIS 3D to determined load-settlement curve for both surface and embedded eccentrically loaded circular footings.

CHAPTER 3

MATERIAL USED

AND EXPERIMENTAL

PROCEDURE

3.1 Introduction

So as to study the bearing capacity of eccentrically loaded Circular footing on granular soil (sand), the experimental program was designed. To fill this need, the laboratory model tests were conducted on circular footings in 69% relative density, load eccentricity (e) was varied from 0 to $0.15B$ (B = Diameter of circular footing) at an increment of $0.05B$, and the depth of embedment (D_f/B) was varied from 0 to 1.0 at an increment of 0.5. The ultimate bearing capacity was interpreted from every test and investigated.

3.2 Material

- Sand
- Circular footing(Diameter(B)=100mm, thickness (t)=25mm)

3.2.1 Sand

The sand utilized as a part of experimental program was collected from the river bed of Koel River. By quick washing and cleaning, it is made free from roots, organic matters etc. The collected sample was sieved to get the required grading by passing through 710 micron and retained at 300 micron. As dry sand does not include the effect of moisture, it can be used as soil medium for the test. Table 3.1 shows the Geotechnical properties of the sand. The curve of grain size distribution is plotted in Figure 3.1. All the experiment were conducted over sand with 69% relative density. The unit weight for 69% relative density is 14.32 kN/m^3 and the friction angle of sand is 40.8° which obtained from direct shear tests.

3.2.2 CHARACTERISTICS OF SAND

Table 3.1: Geotechnical property of sand

| Property | Value |
|---------------------------------------|----------------|
| Specific gravity (G) | 2.63 |
| Effective particle size (D_{10}) | 0.350mm |
| Mean particle size (D_{50}) | 0.44mm |
| Uniformity coefficient (C_u) | 1.30 |
| Coefficient of curvature (C_c) | 1.11 |
| Working dry density (d) | 14.32 kN/m^3 |
| Maximum unit weight ($d_{(max)}$) | 15.08 kN/m^3 |
| Minimum unit weight ($d_{(min)}$) | 12.90 kN/m^3 |
| Relative Density (D_r) | 69% |
| Internal angle of friction (ϕ) | 40.8° |

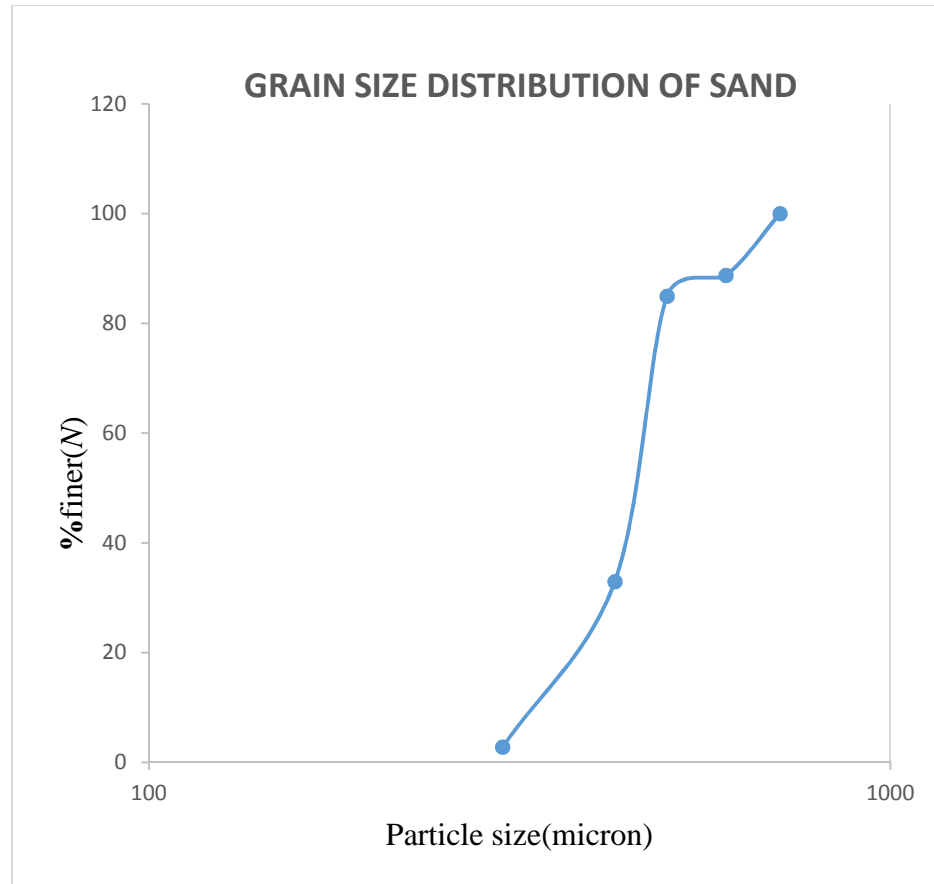


(Figure 3.1: Grain Size Distribution of Sand)

3.3 Experimental procedure

The model tests were conducted in a mild steel tank measuring 1.0m (length) \times 0.504m (width) \times 0.655m (height). To avoid bulging during test all four side of tank are braced. The tank two length sides are made with high strength fiberglass of 12mm thickness. Circular type model foundation have been taken, having dimension 100mm (width B) 25mm (thickness t) which made up of mild steel plate. Glue applied at bottom of footing and then rolling the model footing on sand to made rough bottom. For achieve required relative density Sand was poured in layer of 25mm into the test tank from a fixed height by raining technique. Several trials made in the test tank to maintain height of fall prior to the model test for achieved the desired unit weight. The model foundation

was putted at a desired D_f/B ratio at the middle of the tank. Load to the model foundation was applied by a loading assembly manually. Given Fig 3.2 and Fig. 3.3 shows the photographic image of experimental setup of surface and embedded condition laboratory model tests. The load applied to the model foundation is measured by Proving ring (10KN with 12.121N least count). Settlement of the model foundation is measured by dial gauges (.01mm least count range 50mm) placed on two edges along the width side of the model foundation. Figure 3.2 shows the photographic image of prepared sand sample with two dial gauges arranged diagonally over the Circular footing for the test.



Figure3.2: Experimental setup of laboratory model tests at Surface condition



Figure 3.3: Experimental setup of laboratory model tests at embedded condition

3.4 Model test series

Table 3.2: Model test series for experiment

| Test series | D_f/B | B/L | e/B |
|-------------|---------|-------|------------------|
| 1-4 | 0 | 1 | 0,0.05,0.10,0.15 |
| 5-8 | 0.5 | 1 | 0,0.05,0.10,0.15 |
| 9-12 | 1 | 1 | 0,0.05,0.10,0.15 |

CHAPTER 4

EXPERIMENTAL

RESULTS

AND ANALYSIS

4.1 Introduction

The laboratory model test have been conducted by using circular footing with the eccentricity ratio e/B varying from 0 to 0.15 and embedment Ratio D_f/B varying from 0 to 1, The effect of load eccentricity on the load carrying capacity of Circular embedded footings was investigated from the tests, dry sand bed used for laboratory model test.

4.2 Centric loading conditions

The model tests are performed in centric vertical loading condition (i.e. $e/B = 0$). Basically, the ultimate bearing capacity is determined by Tangent Intersection method for present test. There are five different method to calculate ultimate bearing capacity from the load-settlement curve i.e. Break Point method (Mosallanezhad et al. 2008). Tangent Intersection method (Trautmann and Kulhawy 1988), 0.1B method (Briaud and Jeanjean 1994), Log-Log method (DeBeer 1970), and Hyperbolic method (Cerato2005),

Table 4.1: Model test parameters for the case of Centric Loading condition

| B/L | Sand type | Unit weight (kN/m^3) | Relative Density of Sand % | Friction angle Direct shear test (Degree) | D_f/B | e/B |
|-------|-----------|-----------------------------|----------------------------|--------------------------------------------------|---------------|-------|
| 1 | Dense | 14.32 | 69 | 40.8 | 0 0.5 1 | 0 |

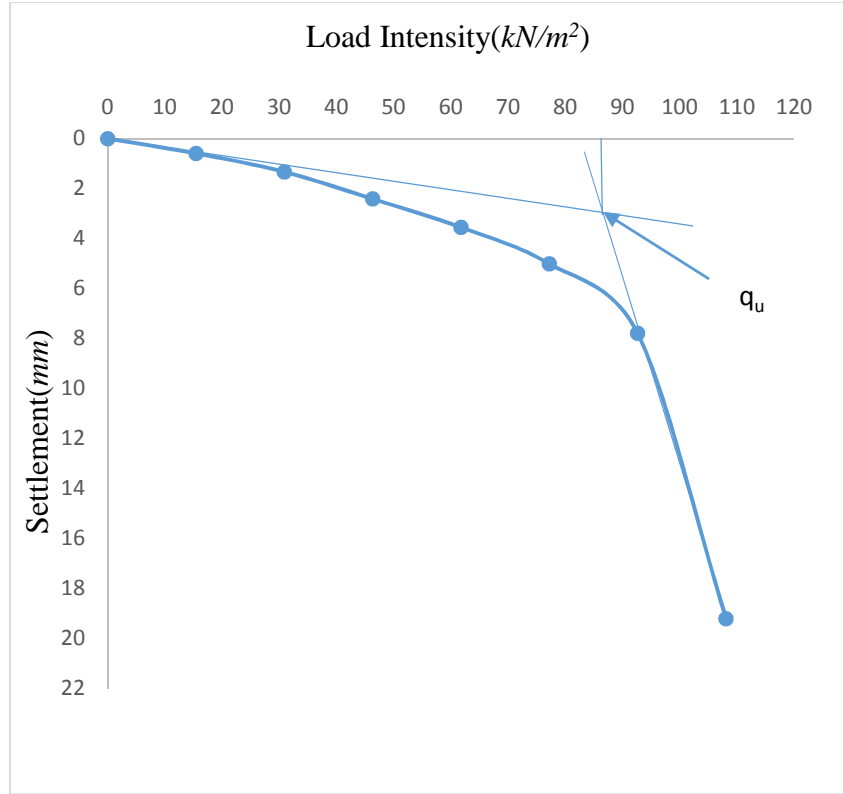


Figure 4.1: Interpretation of Ultimate Bearing Capacity q_u by Tangent Intersection method

4.2.1 Surface Footing with Centric Loading Conditions

Definite failure point is observed for central loading condition with circular footing of size (10cm diameter). The characteristics of General shear failure shown by this curve. Tangent intersection method is used to obtain ultimate bearing capacity of footing. From the load settlement curve of centrally loaded circular footing ultimate bearing capacity, q_u is 87 kN/m^2 .

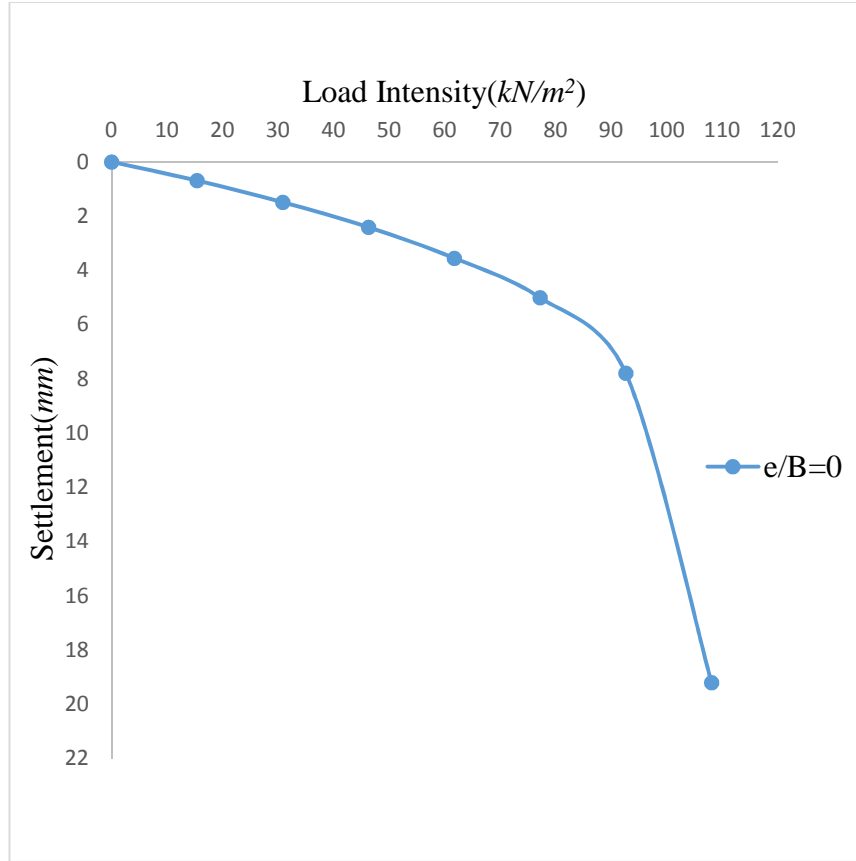


Figure 4.2: Load Settlement curve with $D_f/B=0$, $e/B=0$

4.2.2 Embedded Footing at Centric Loading Conditions

Load settlement curves are obtained from the experimental results for different D_f/B ratio (0, 0.5, and 1). The combined load settlement curves of $D_f/B=0, 0.5, 1.0$ are shown in Fig. 4.3. As seen from figure the bearing capacity of circular footing increases with the increase in depth of embedment. The ultimate bearing capacity for 0.5B depth of embedment is $160 kN/m^2$ at centric condition (i.e. $e/B=0$). Similarly for 1B depth of embedment at centric loading condition the ultimate bearing capacity is $230 kN/m^2$.

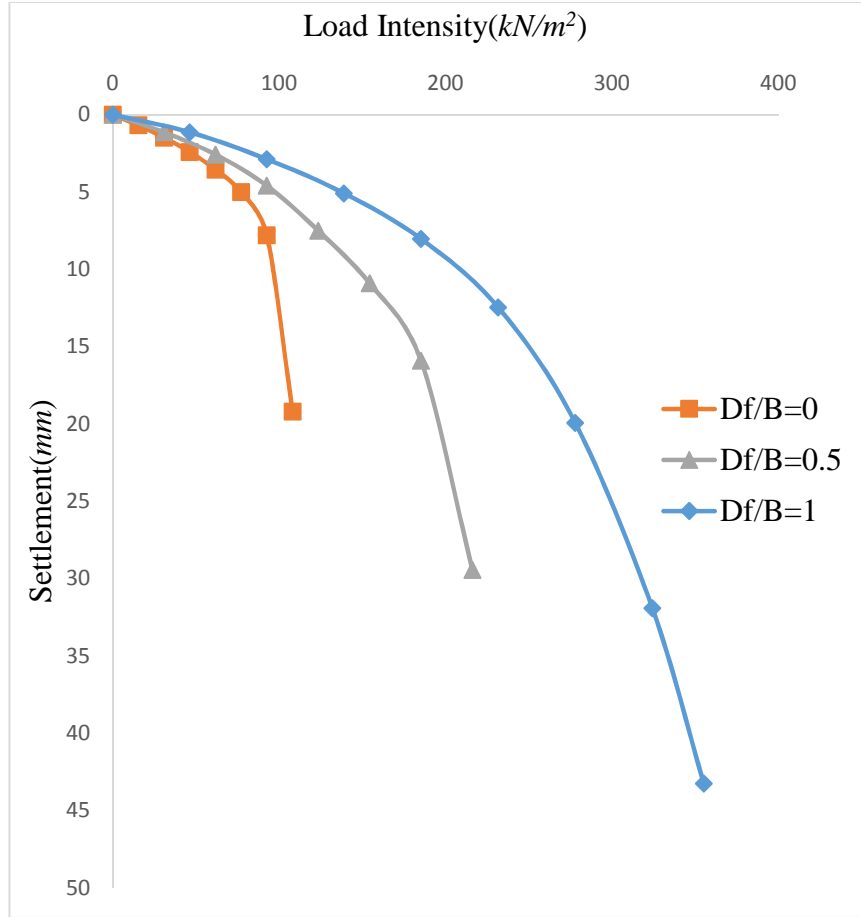


Figure 4.3: Variation of Load-Settlement Curve with Embedment ratio (D_f/B) at $e/B=0$

For the case of centric loading ($e/B = 0$) at various depth to width ratio t i.e. $D_f/B = 0, 0.5$ and 1.0 the theoretical values of ultimate bearing capacities corresponding to $\phi = 40.8^\circ$ have been obtained using the various theory of Meyerhof (1963), Terzaghi (1943), Hansen (1970), Vesic (1973), IS code (6403-1983). These values are plotted in Fig. 4.4 the same has been presented in Table 4.2, which represent the present experimental values along with the theoretical values.

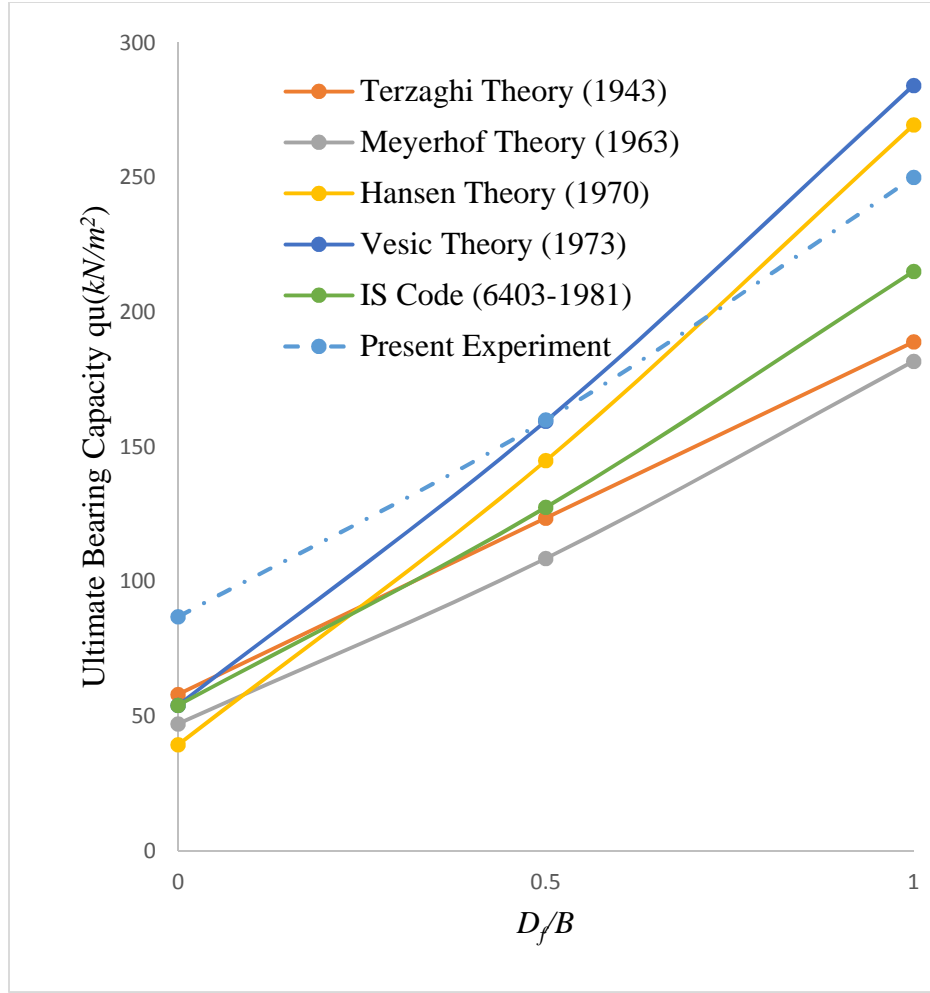


Figure 4.4: Variation of q_u with D_f/B for $e/B = 0$ using formulae of existing theories along with present experimental values

It is investigated from the Fig. 4.4 the bearing capacities obtained experimentally is significantly higher than those predicted by theories except Hansen and Vesic method for given condition of embedment due to the shape and depth factor. Geotechnical laboratories clearly shows that model test results for model tests of bearing capacity for shallow foundation are, in general, much higher than those calculated by traditional methods. The most important reason among several reason for this is the unpredictability of N_γ and the model test scale effect. Several bearing capacity test results which shown in Fig 4.5 as plot of N_x vs. x/B predicted by DeBeer (1965). The N_x value rapidly

decreases with the increase in γB value. The variation of N_γ obtained from small scale laboratory and large scale field test results also compared, and these are given in Fig. 4.5

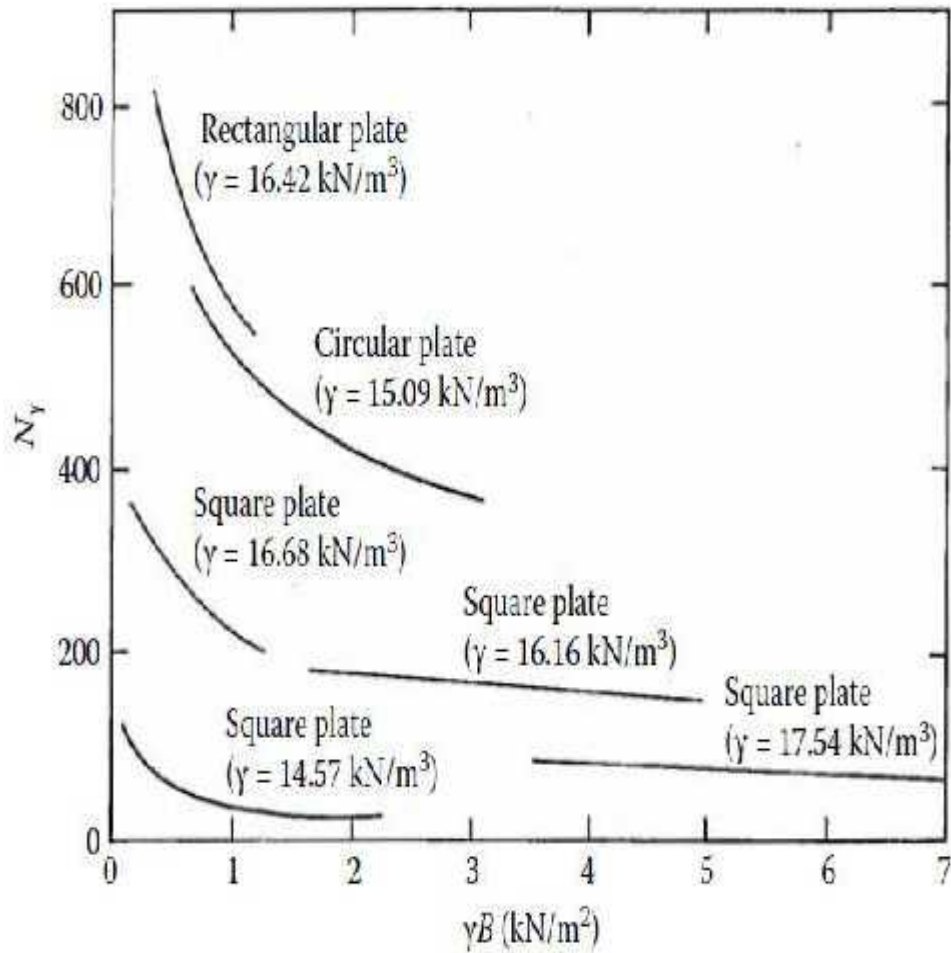


Figure 4.5: Variation of N with B (adapted after DeBeer, 1965)

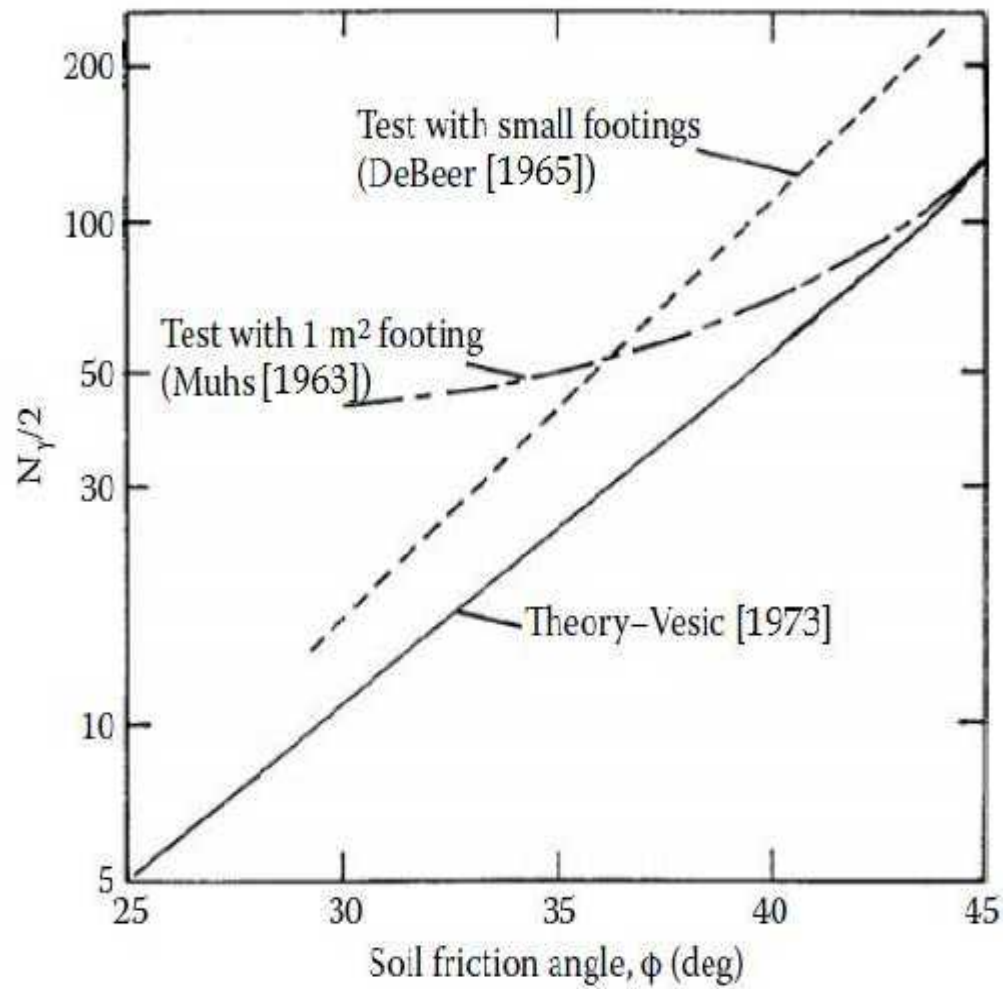


Figure 4.6: Comparison of N obtained from tests with small footings and large footings of 1m² area on sand (adapted after DeBeer, 1965).

Table 4.2: Calculated values of ultimate bearing capacities q_u by different theories along with present experimental value

| e/B | D_f/B | Present Experiment; $q_u(kN/m^2)$ | Terzaghi (1943); $q_u(kN/m^2)$ | Meyerhof (1963); $q_u(kN/m^2)$ | Hansen (1970); $q_u(kN/m^2)$ | Vesic (1973); $q_u(kN/m^2)$ | Is code(6403- 1981); $q_u(kN/m^2)$ |
|-------|---------|-------------------------------------------------------------|----------------------------------------------------------|----------------------------------------------------------|--------------------------------------------------------|-------------------------------------------------------|------------------------------------------------------------------|
| 0 | 0 | 87 | 58.19 | 47.22 | 39.49 | 54.15 | 54.15 |
| 0 | 0.5 | 160 | 123.59 | 108.61 | 144.90 | 159.56 | 127.57 |
| 0 | 1 | 230 | 188.98 | 181.82 | 269.49 | 284.15 | 215.14 |

4.3 Eccentric Loading Conditions

Twelve numbers of model tests are conducted in eccentric loading condition. The load settlement curves of Circular foundations ($e/B = 0, 0.05, 0.1$ and 0.15) in surface condition are plotted in Fig. 4.7. The load carrying capacity decreases with increase in e/B ratio. Similarly, the variation of load-settlement curve with depth of embedment (D_f/B) shows by Fig.4.10 to Fig. 4.12

4.3.1 Surface Footing at Eccentric Loading Conditions

The ultimate bearing capacity of Circular footings with eccentric loading of ($e/B = 0, 0.05, 0.1$, and 0.15) has been found out. The values obtained are presented in Table 4.4 and shows in Fig.4.7. Similarly, for surface circular footing with load eccentricities the ultimate bearing capacities have been computed and shown in Fig. 4.7. It is found that for eccentric loading $e/B=0.05, 0.1, 0.15$ the

ultimate bearing capacities are 78 kN/m^2 , 60 kN/m^2 and 52 kN/m^2 respectively. It is observed that the UBC decreases with increase in eccentricity.

Table 4.3: Model test parameters for the case of Eccentric Loading condition

| B/L | Sand type | Unit weight (kN/m^3) | Relative Density of Sand % | Friction angle Direct shear test (Degree) | D_f/B | e/B |
|-------|-----------|------------------------------------|----------------------------|--------------------------------------------------|---------|-------|
| 1 | Dense | 14.32 | 69 | 40.8 | 0 | 0 |
| | | | | | 0.5 | 0.05 |
| | | | | | 1 | 0.1 |
| | | | | | | 0.15 |

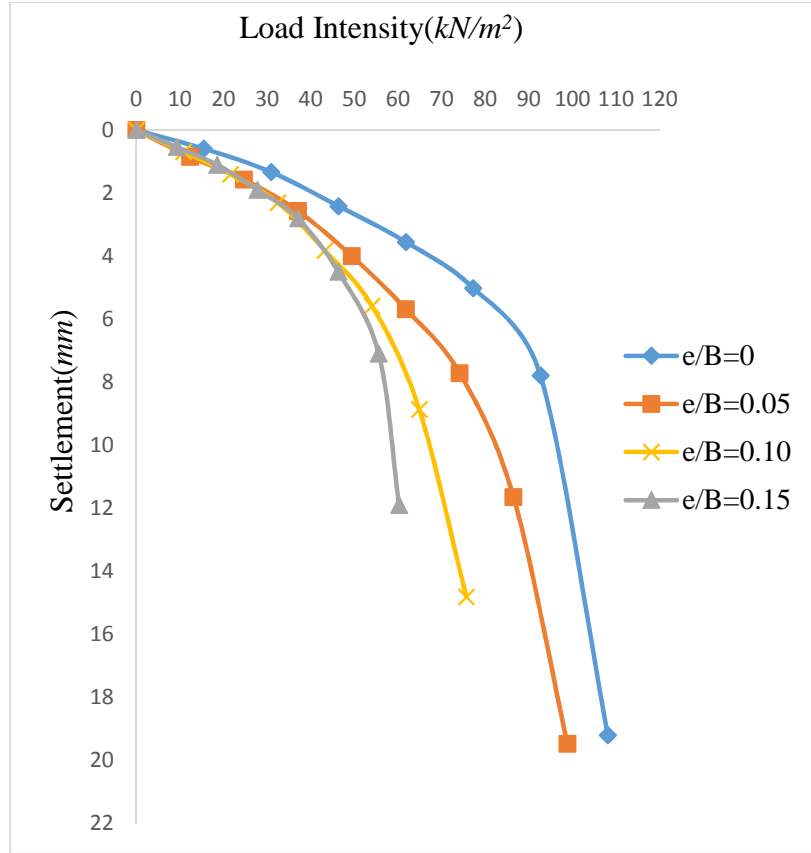


Figure 4.7: Load Settlement Curve with $D_f/B=0$, $e=0, 0.05B, 0.10B, 0.15B$

4.3.2 Embedded Footing at Eccentric Loading Conditions

In order to show the effect of embedment and effect of eccentricity, load-settlement curves have been plotted for the case of eccentrically embedded footing. At a depth of embedment equal to $0.5B$ or $1.0B$, the bearing capacity decreases with increase in eccentricity like surface footing at any settlement level. It is seen that the ultimate bearing capacity of footing increases with the increase in depth to width ratio of footing at any eccentricity. Similarly, at any depth of embedment, the ultimate bearing capacity decreases with increase in eccentricity. The values obtained are presented in Table 4.4. The same has been shown in Fig. 4.8 and 4.9.

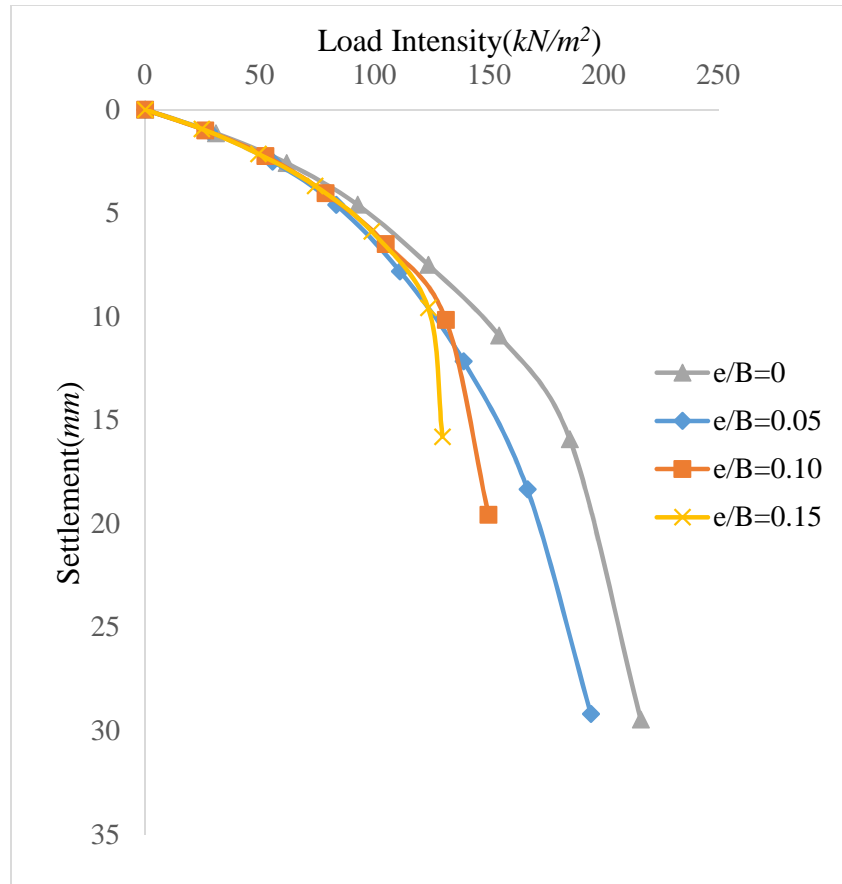


Figure 4.8: Load-Settlement Curve with $D_f/B=0.5$, $e=0, 0.05B, 0.10B, 0.15B$

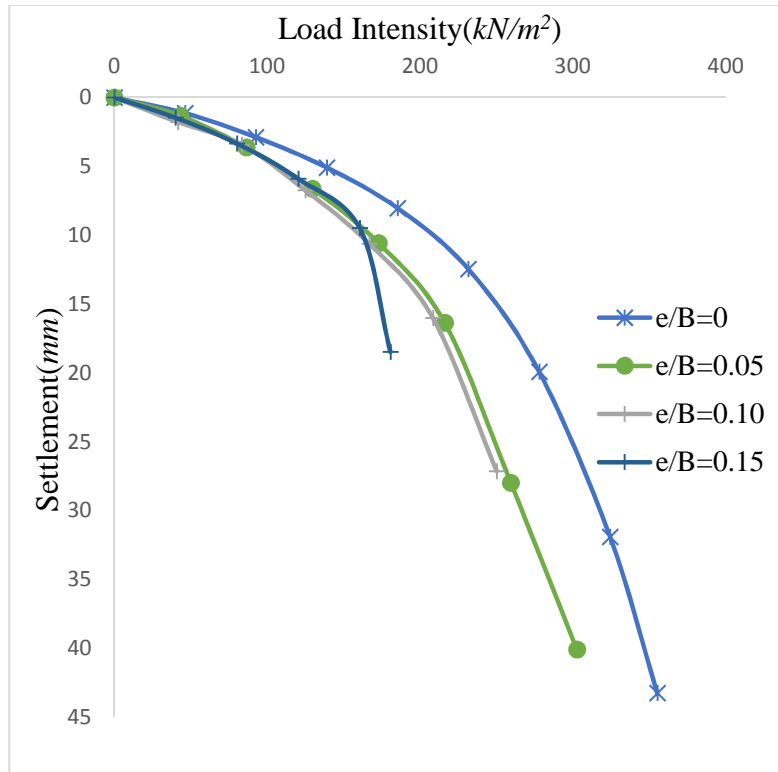


Figure 4.9: Load-Settlement Curve with $D_f/B=1$ $e=0, 0.05B, 0.10B, 0.15B$

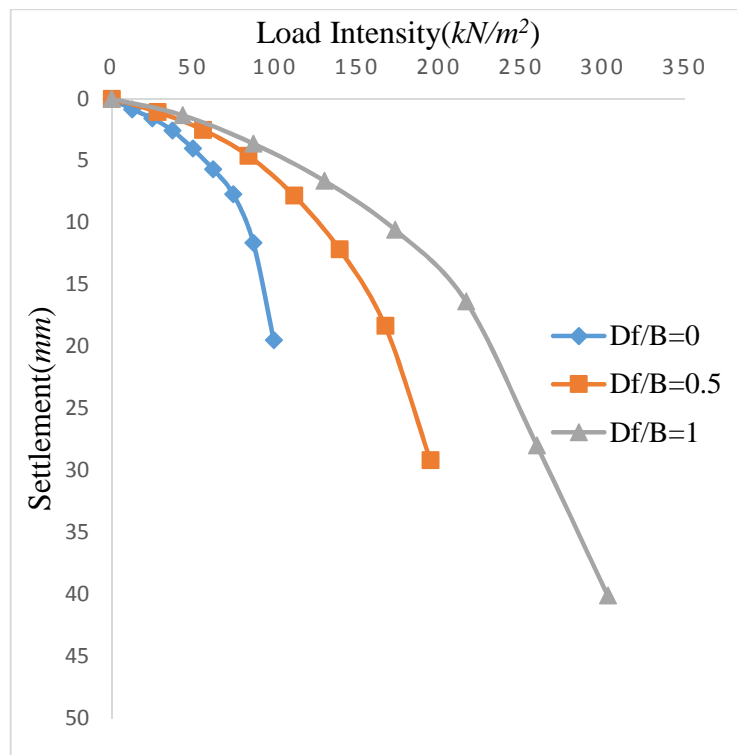


Figure 4.10: Variation of Load-Settlement Curve with Embedment ratio (D_f/B) at $e/B=0.05$

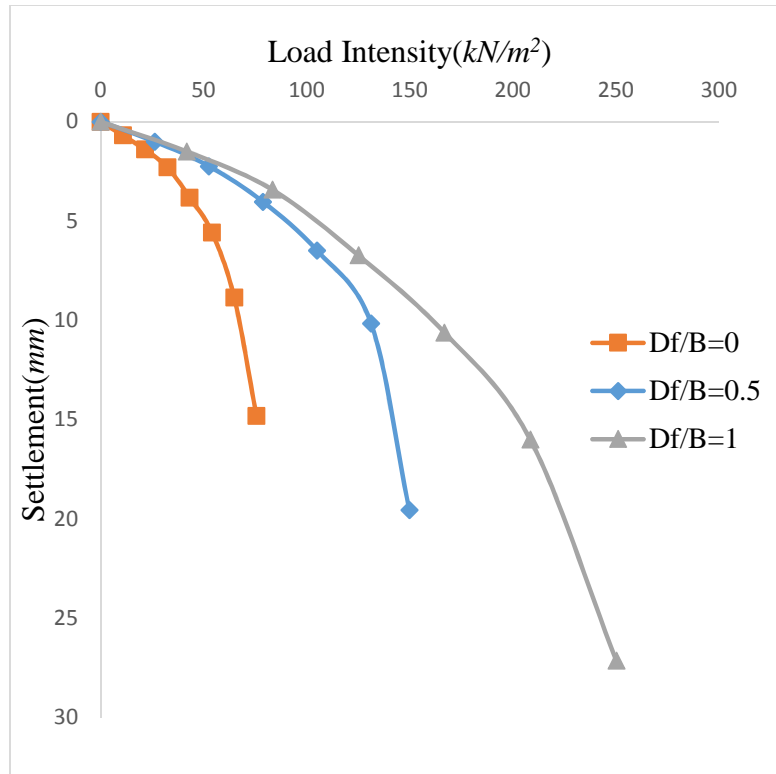


Figure 4.11: Variation of Load-Settlement Curve with Embedment ratio (D_f/B) at $e/B=0.10$

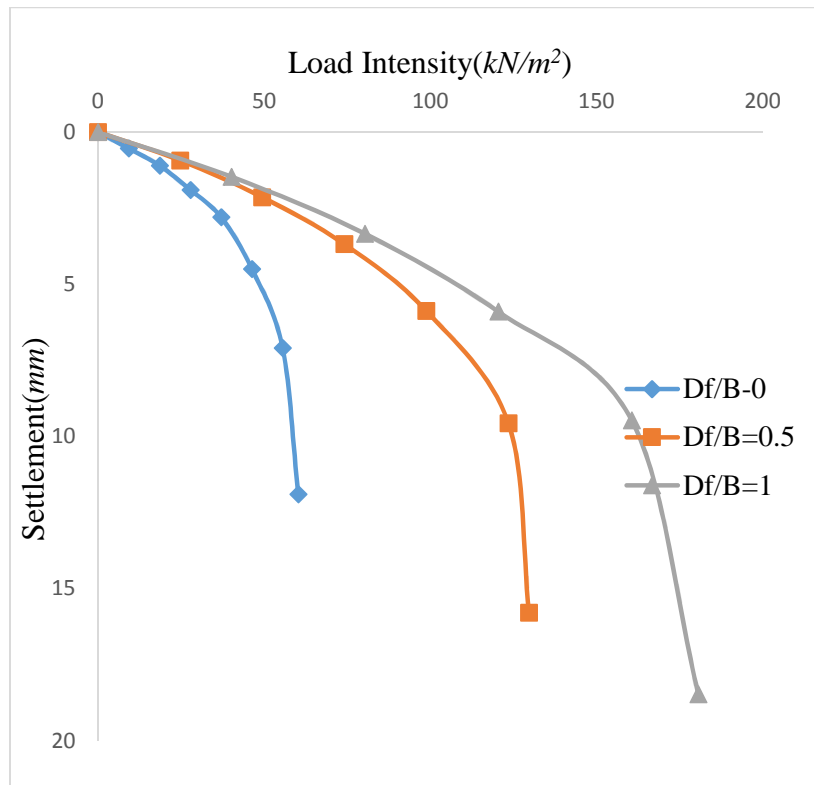


Figure 4.12: Variation of Load-Settlement Curve with Embedment ratio (D_f/B) at $e/B=0.15$

By using Meyerhof's effective area method the experimental ultimate bearing capacities for eccentrically loaded foundations ($e/B = 0, 0.05, 0.1$ and 0.15 , $D_f/B = 0, 0.5$ and 1) are plotted along with the bearing capacities obtained. This is shown in Fig. 4.13 and Table 4.4. The nature of decrement of bearing capacity with the increase in eccentricity as observed from experimental results are with those using Meyerhof's method (1953). It can be seen from Fig.4.13 that the difference in experimental UBC and computed UBC by Meyerhof's method is more at higher eccentricity and higher depth of embedment. Yamamoto and Hira (2009) used finite elements to calculate the bearing capacity of surface foundations on frictional soils under eccentric loadings, and for a friction angle of 35° and an eccentricity $e = (1/3) B$, they found a bearing capacity equal to about 45% of the one determined by the effective width approach. Michalowski and You (1998) also revealed that the effective width rule over- estimates the best upper bound to the average bearing pressure for purely frictional (granular) soil and relatively small surcharge loads. Also for a surface footing with eccentricity $e/B = 0.25$ this overestimation is 35%, and it increases with an increase in e/B .

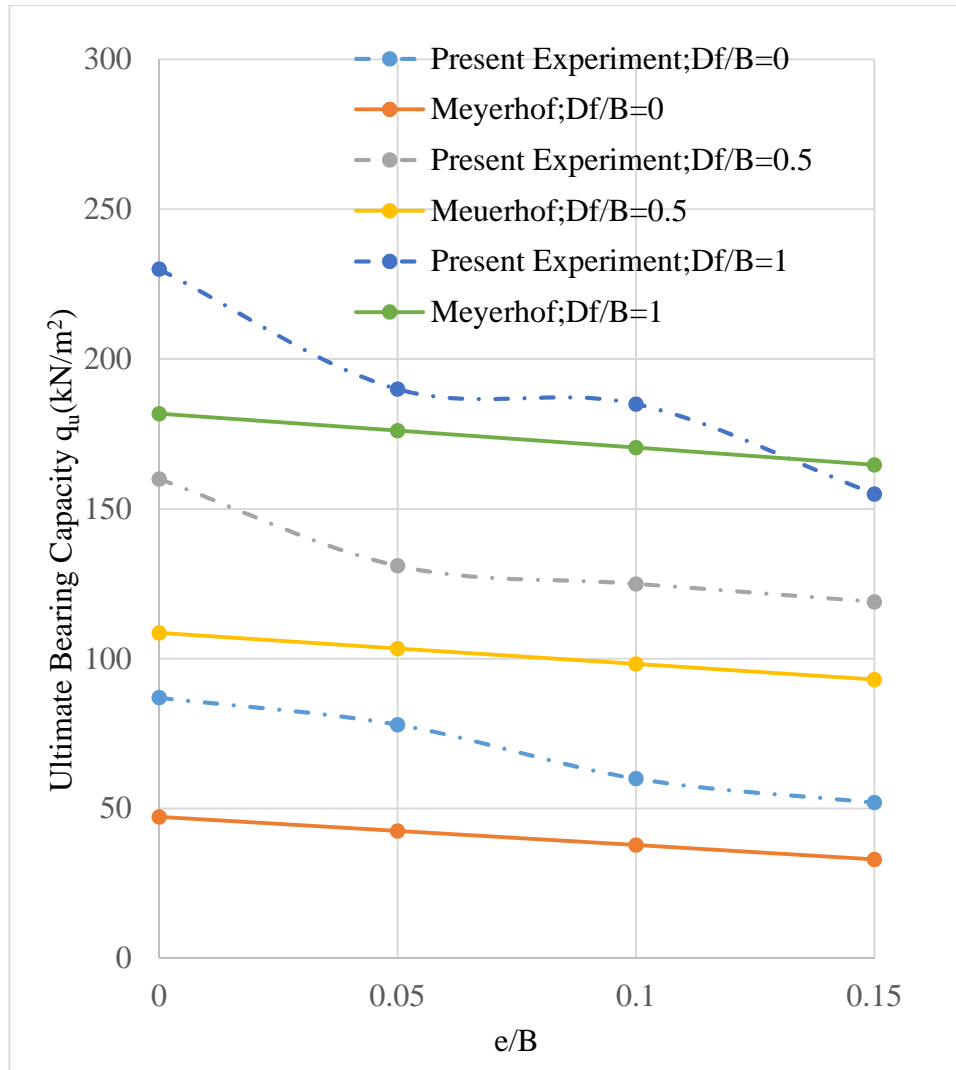


Figure4.13: Comparison of ultimate bearing capacities of Present experimental results
With Meyerhof at different D_f/B and e/B

Table 4.4: Calculated values of (q_u) by Meyerhof (1963) for eccentric condition along with
Present experimental values of q_u

| e/B | D_f/B | Present Experiment; q_u (kN/m^2) | Meyerhof (1963); $q_u(kN/m^2)$ |
|------------|---------------------------|---------------------------------------------------------------------------|----------------------------------------------------------|
| 0 | 0 | 87 | 47.22 |
| 0.05 | 0 | 78 | 42.50 |
| 0.10 | 0 | 60 | 37.78 |
| 0.15 | 0 | 52 | 33.05 |
| 0 | 0.5 | 160 | 108.61 |
| 0.05 | 0.5 | 131 | 103.42 |
| 0.10 | 0.5 | 125 | 98.23 |
| 0.15 | 0.5 | 119 | 93.03 |
| 0 | 1 | 230 | 181.82 |
| 0.05 | 1 | 190 | 176.11 |
| 0.10 | 1 | 185 | 170.40 |
| 0.15 | 1 | 155 | 164.68 |

The reduction factor (RF) obtained from the present experimental data for the Circular footing has been compared with the RF for strip footing as given by Purkayastha and Char at depth of embedment ($D_f/B=0, 0.5, 1.0$). The reduction factors at all eccentricities and at all depth of embedment are not in well close agreement. These are shown in figures 4.14, 4.15 and 4.16

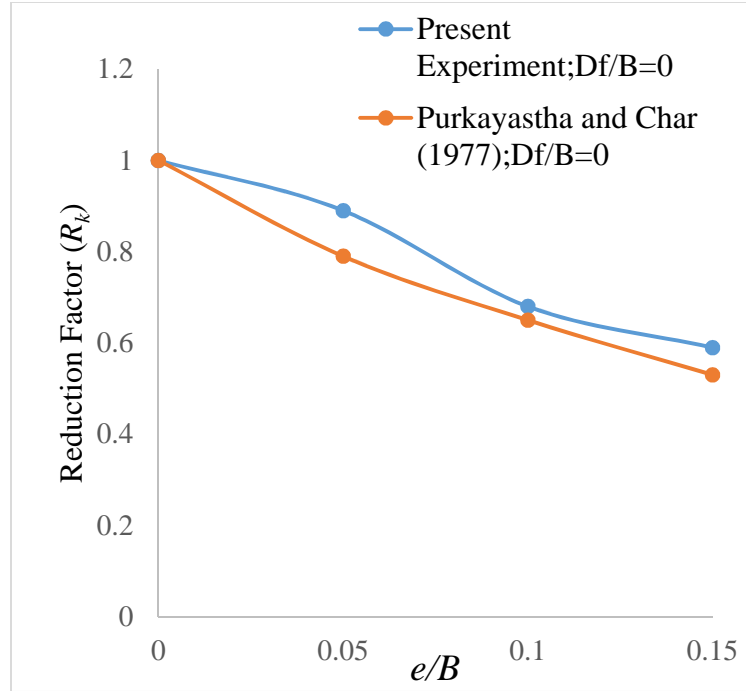


Figure 4.14: Comparison of Present experimental results with Purkayastha and Char (1977) with

$$D_f/B=0$$

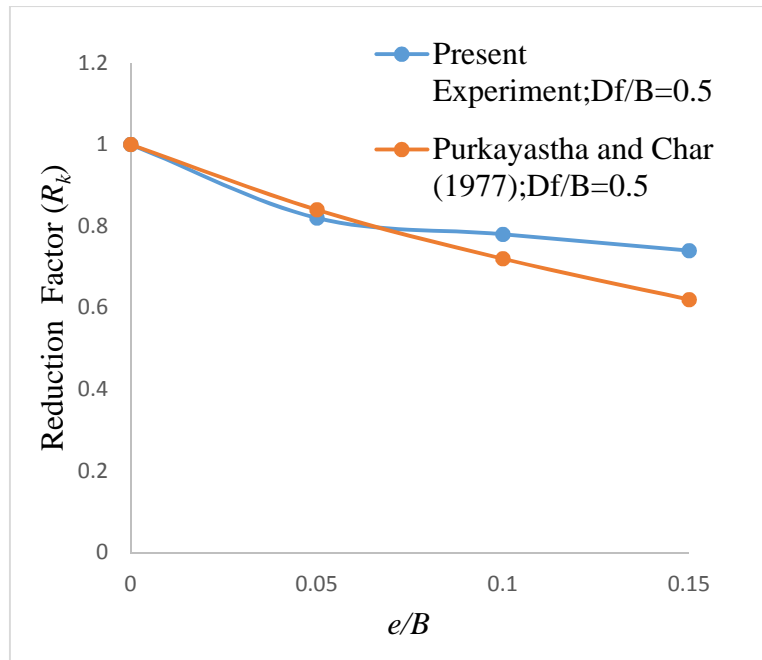


Figure 4.15: Comparison of Present experimental results with Purkayastha and Char (1977) with

$$D_f/B=0.5$$

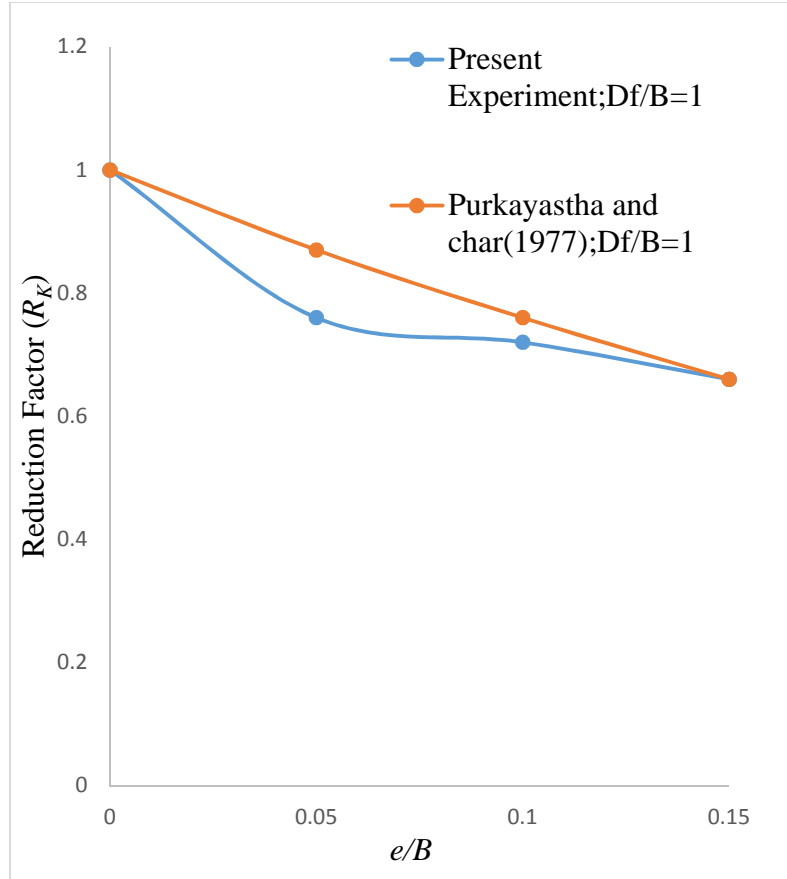


Figure 4.16: Comparison of Present experimental results with Purkayastha and Char (1977)

With $D_f/B=1.0$

Table 4.5: Calculated values of R_k by Purkayastha and Char (1977) for eccentric vertical condition along with Present experimental values.

| D_f/B | e/B | Present Experiment; R_k | Purkayastha and Char (1977); R_k |
|---------|-------|---------------------------------|------------------------------------------|
| 0 | 0 | 1 | 1 |
| 0 | 0.05 | 0.89 | 0.79 |
| 0 | 0.1 | 0.68 | 0.65 |
| 0 | 0.15 | 0.59 | 0.53 |
| 0.5 | 0 | 1 | 1 |
| 0.5 | 0.05 | 0.82 | 0.84 |
| 0.5 | 0.1 | 0.78 | 0.72 |
| 0.5 | 0.15 | 0.74 | 0.62 |
| 1 | 0 | 1 | 1 |
| 1 | 0.05 | 0.76 | 0.87 |
| 1 | 0.10 | 0.74 | 0.76 |
| 1 | 0.15 | 0.62 | 0.66 |

CHAPTER 5

SUMMERISED

EXPERIMENTAL

RESULTS

5.1 Conclusion

Following are the conclusions drawn from the investigation which is according to the laboratory experiments.

- Ultimate bearing capacity of circular footing is effected by the depth of embedment (D_f/B) and to the eccentricity ratio (e/B) of foundation.
- Ultimate bearing capacity decreases by increasing the eccentricity (e/B) ratio for both surface and embedded condition.
- The ultimate bearing capacity by reduction factor developed from present experiments is in well compared with existing theory by Purkayastha and char (1977).
- For the eccentric loaded circular footing the Bearing Capacity increases with increase in embedment.
- Settlement of circular foundation increases by increasing embedment (D_f/B) ratio.

CHAPTER 6

NUMERICAL

ANALYSIS

6.1 Introduction

PLAXIS is a FEM package used for analysis of stability and deformation of structure. It is developed at the Technical University of Delft. At the initial stage, this was used to analyse the soft soil river embankments of the lowlands of Holland. But later, a company named PLAXIS BV was formed, and expansion of the program was done to address a wide range of geotechnical issues. It requires advanced and anisotropic behaviour of soils and rock for analysis purpose. As soil being a material with multiple phases, some additional methods are adopted to take care of hydrostatic and non-hydrostatic pore pressures within the soil. Here, the modelling of the soil is an important aspect. But many projects require the modelling of structures and the interaction between soil and structure. PLAXIS is a software package well equipped with advanced features to deal with complex problems involved in geotechnical engineering. There are two different approaches: experimentally, by conducting model and full-scale tests; or, analytically, by using methods such as finite elements used to solve the foundation engineering problem. Full-scale tests are the ideal method for obtaining data, however, practical difficulties and economic considerations either eliminate or considerably restrict the possibility of full-scale testing. As an alternative model tests may be employed, but they have disadvantages. Boundary conditions, the size of the footing, the sample disturbance, the test setup and procedure of the testing box usually affected the model tests results. Due to the fortunate developments in numerical methods and computer programming, it is advantageous to use these techniques to simulate the conditions of model tests to verify the theoretical models. The theoretical study can then be extended to cover a wide range of field cases which engineers omitted using full-scale testing.

In the present study, the program “PLAXIS 3D” used for Numerical analysis. It is a finite-element based software. The stresses, strains and failure aspects of a given problem can be evaluated by using this software.

6.2 METHODOLOGY

The finite element program PLAXIS 3D (version 2013), is used to model the tests of circular footing on granular sand. PLAXIS is intended for the analysis of deformation and stability in geotechnical engineering projects. The Mohr–Coulomb model is used for soil and linear-elastic model is used for the footing; undrained behavior is adopted for the analysis and 10-node tetrahedral elements are used for the analysis. Elastic modulus of sand (E) is calculated from stress strain curve (Lysandros pantelidis 2005). The parameters used in the analysis are tabulated in below Table

Table 6.1: Parameter used in numerical analysis

| Parameter | Value |
|------------------------------------------------------|-----------------|
| Angle of internal friction (ϕ) ($^{\circ}$) | 40.8 |
| Unit weight of sand (kN/m^3) | 14.32 |
| Unit weight of steel (kN/m^3) | 78.5 |
| Poisson's ratio () | 0.33 |
| Modulus of elasticity of sand (E) (kN/m^2) | 9000 |
| Modulus of elasticity of steel(E) (kN/m^2) | 2×10^8 |
| Dilatancy angle ($^{\circ}$) | 10.8 |
| Relative density of sand (D_r) (%) | 69 |
| Cohesion C (kN/m^2) | 0 |

6.2.1 Testing procedure

First a geometric model of dimension 1m x 0.5m x 0.655m is created. The footing of size (0.1m diameter and 0.025m thickness) is placed on the top surface of the soil model at desired position at the center or a distance away from it according to different eccentricities. A very fine mesh is generated in the geometry. An incremental vertical load is applied on the surface of the footing, according to different loading conditions. Then the loading point of the soil model is selected for the analysis. The calculations are done until the failure of the soil. The load- settlement curve obtained from the output gave the ultimate bearing capacity of the circular footing by using tangent intersection method for different loading conditions. Same procedure is adopted for different loading conditions. Given Fig.6.1 shows the general procedure of analysis

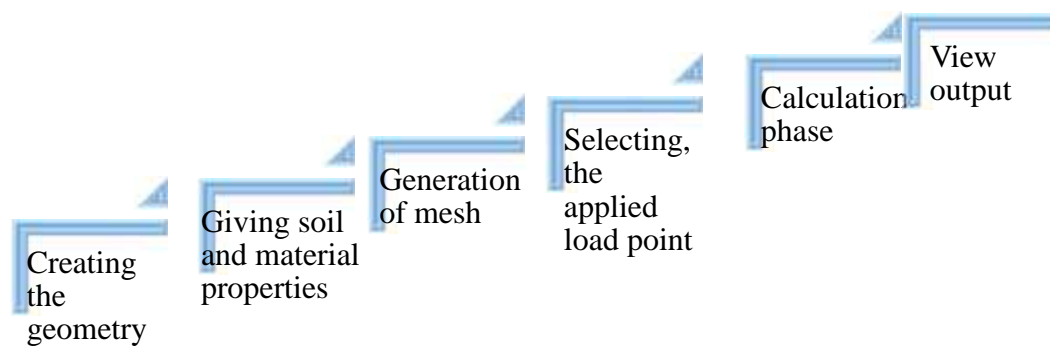


Figure 6.1: General procedure of analysis

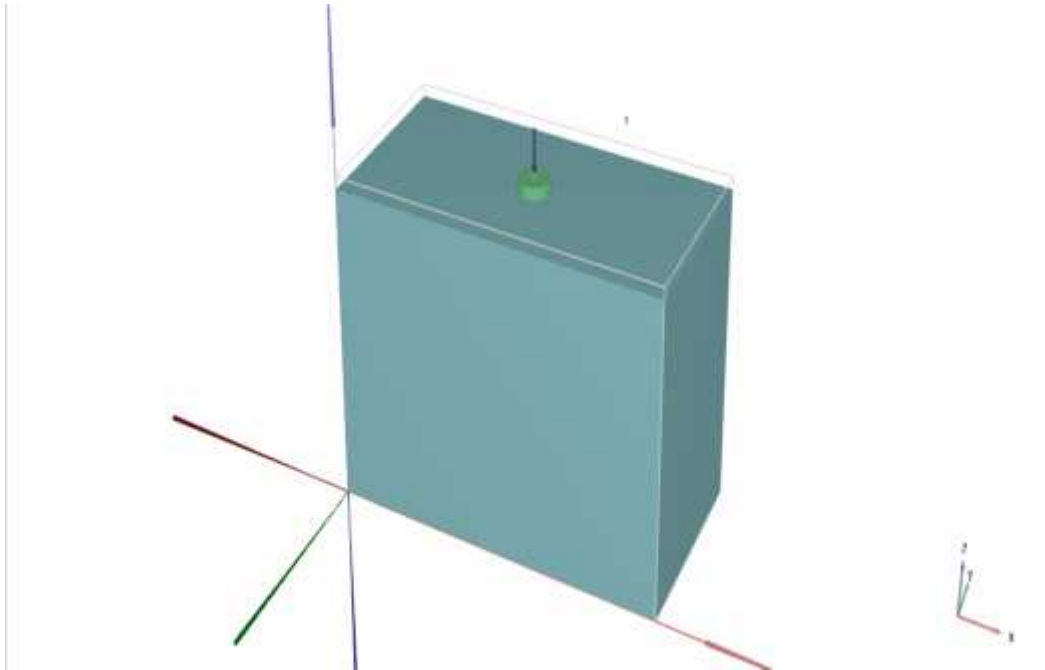


Figure 6.2: Geometry model for analysis at surface condition ($e/B=0$)

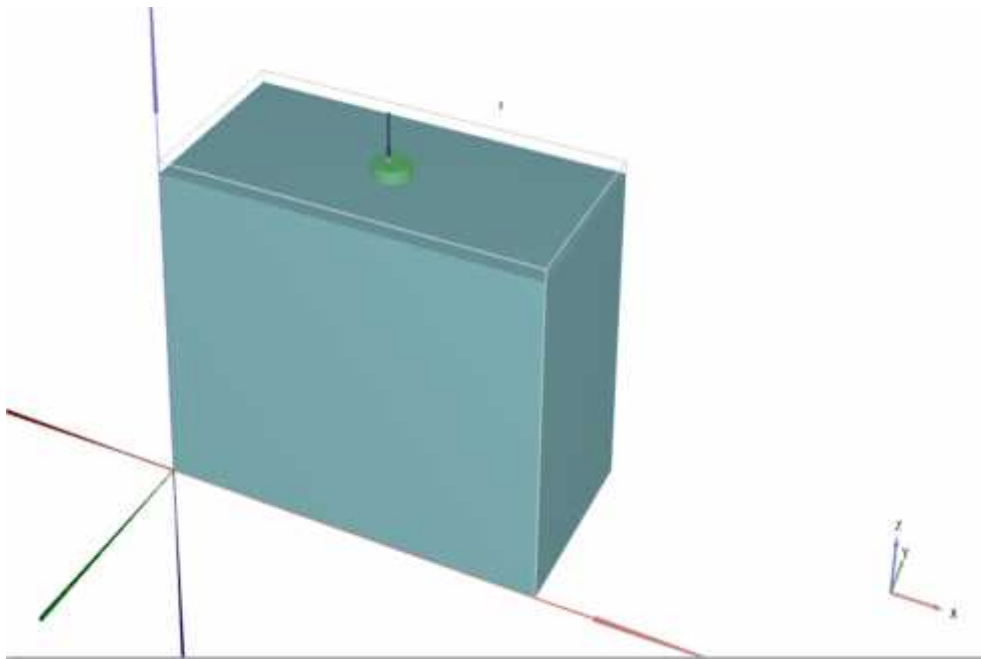


Figure 6.3: Geometry model of eccentrically loaded footing at ($D_f/B=0$, $e/B=0.15$)

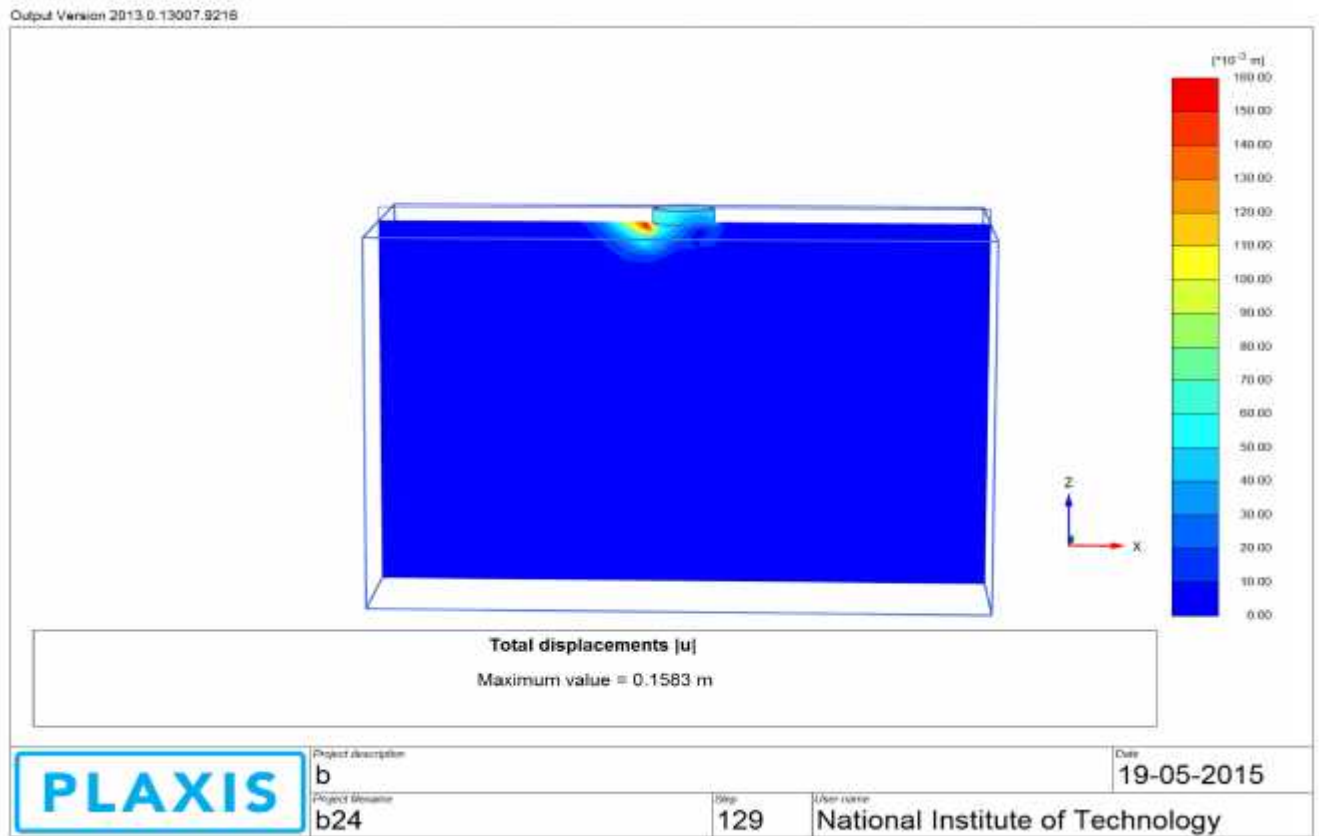


Figure 6.4: Failure pattern at eccentric condition ($e/B=0.15$)

6.3 Results analysis

Numerical analysis have been occurred over unreinforced soil with circular footing by using PLAXIS 3D. The result has been investigated for surface case ($D_f/B=0$) and embedded case of ($D_f/B=0.5, 1.0$) along with different eccentric condition ($e/B=0, 0.05, 0.10, 0.15$). The load settlement curve for surface condition at different eccentric ratio shown by Fig.6.7. Fig. 6.9 shown the load settlement curve for embedded condition at different eccentric ratio. For both the cases

ultimate bearing capacity decreases by increasing eccentricity. By increasing embedment ratio ultimate bearing capacity increases.

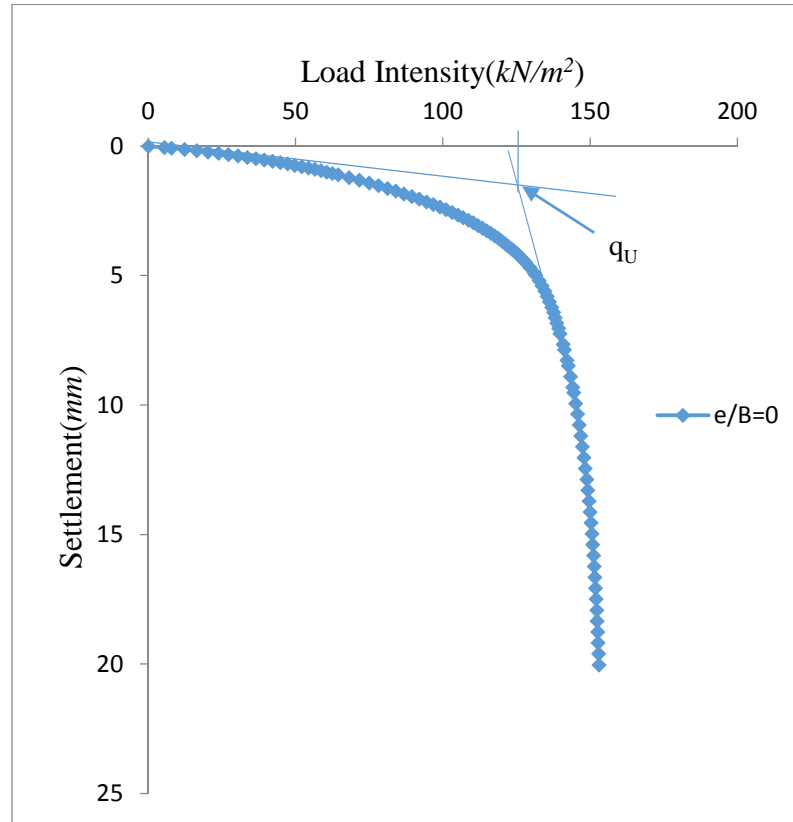


Fig.6.5: q_u value shown by tangent intersection method at $e/B=0$, $D_f/B=0$

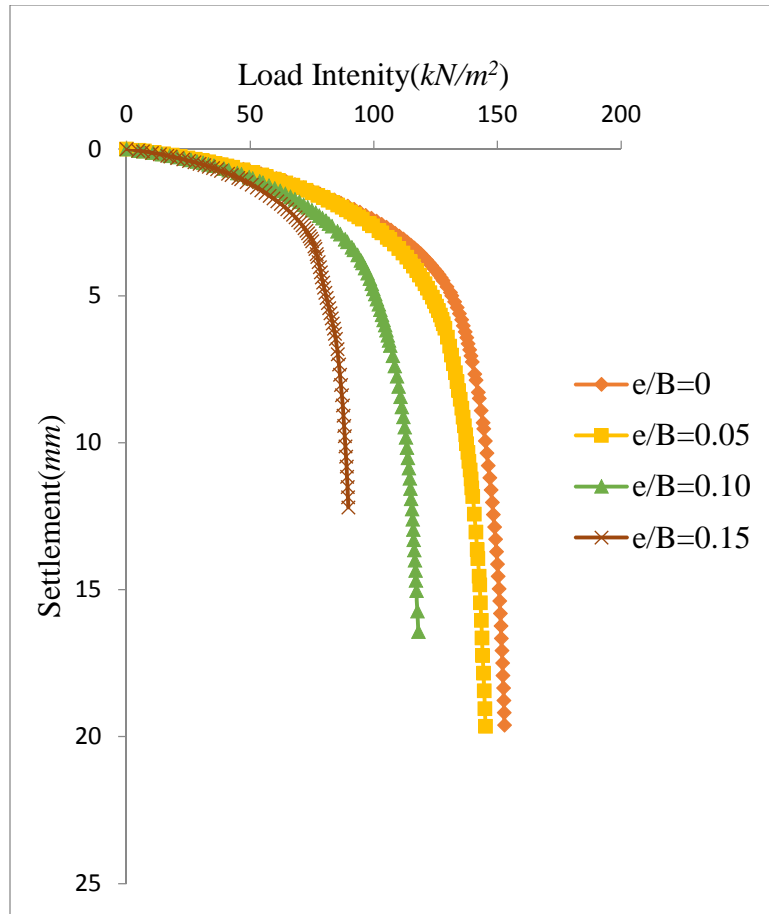


Figure 6.6: Variation in Load settlement curve at $D_f/B=0$

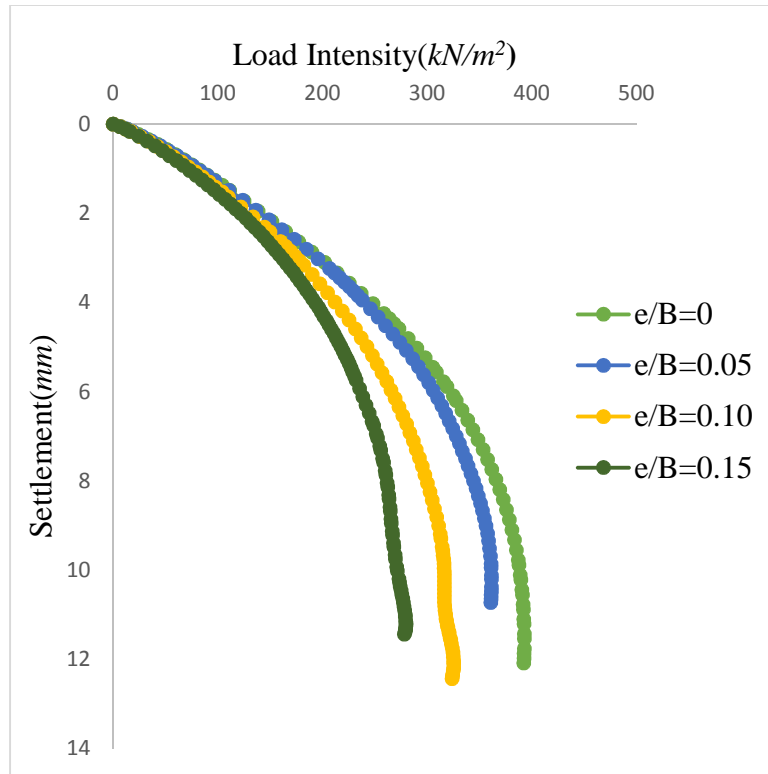


Figure.6.7: Variation in Load settlement curve at $D_f/B=0.5$

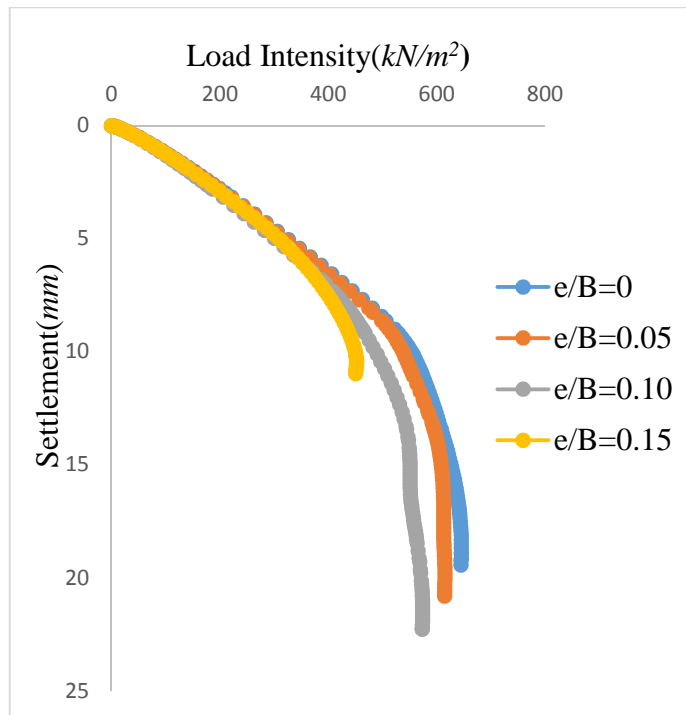


Figure 6.8: Variation in Load settlement curve at $D_f/B=1$

6.3.1 Comparison

Fig.6.9 to Fig. 6.12 shown the load settlement compared curve for some cases obtained by both experimental and numerical analysis by using circular footing. Almost same pattern observed in comparison. The value of q_u obtained numerically higher then experimental due to the soil parameter such as elasticity modulus used in analysis and the displacement value obtained in the laboratory. There is good compatibility of observation between experiment and numerical analysis.

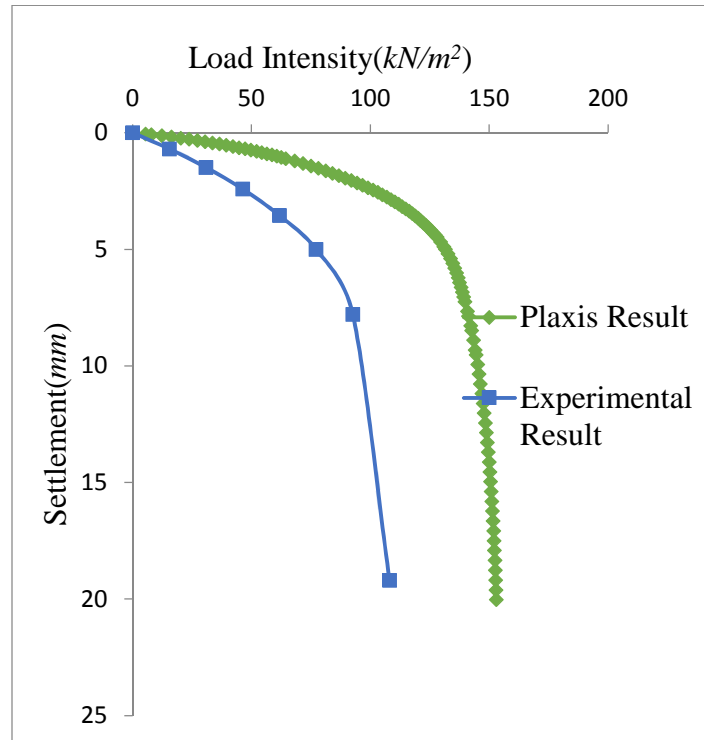


Figure 6.9: Comparison Load settlement curve at $D_f/B=0$, $e/B=0$

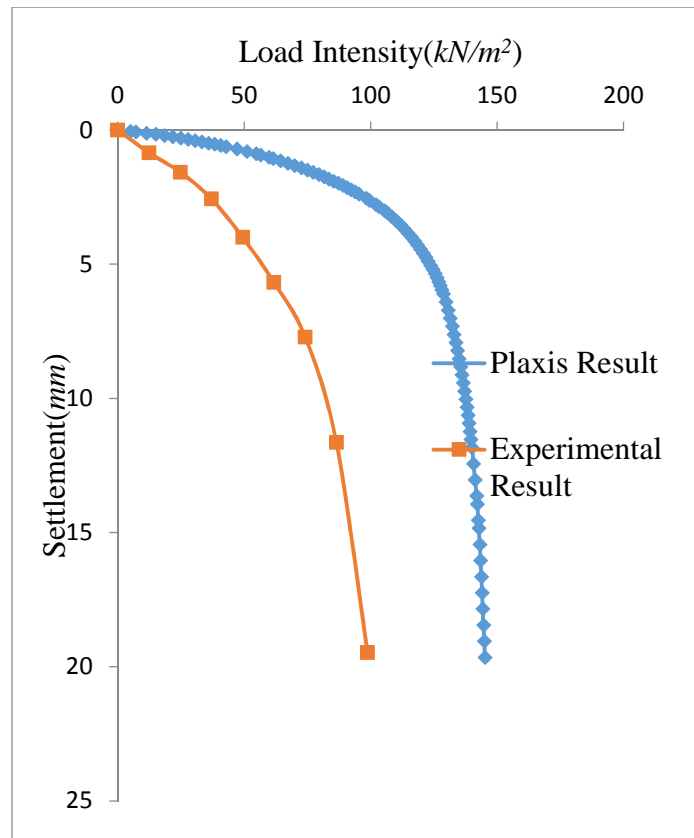


Figure 6.10: Comparison Load settlement curve at $D_f/B=0$, $e/B=0.05$

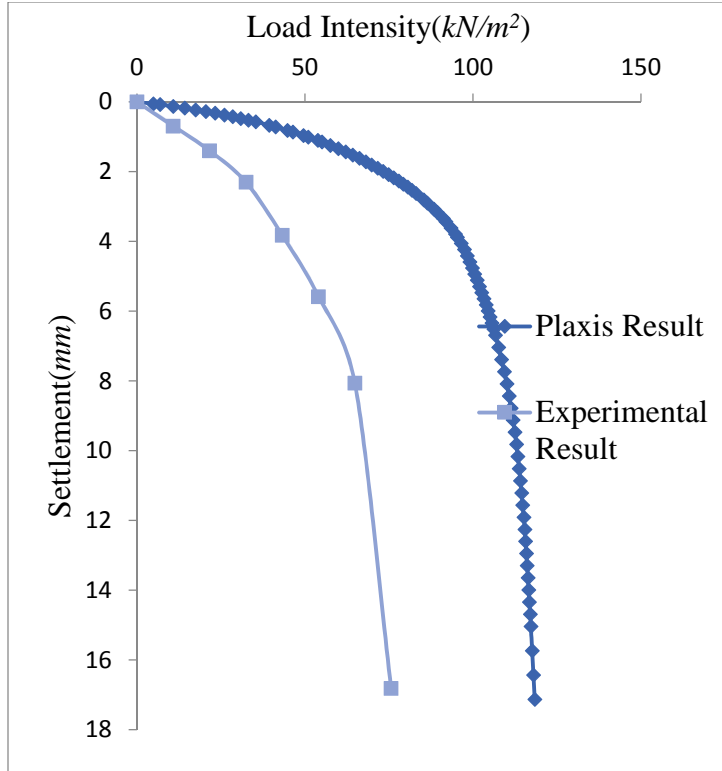


Figure 6.11: Comparison Load settlement curve at $D_f/B=0$, $e/B=0.10$

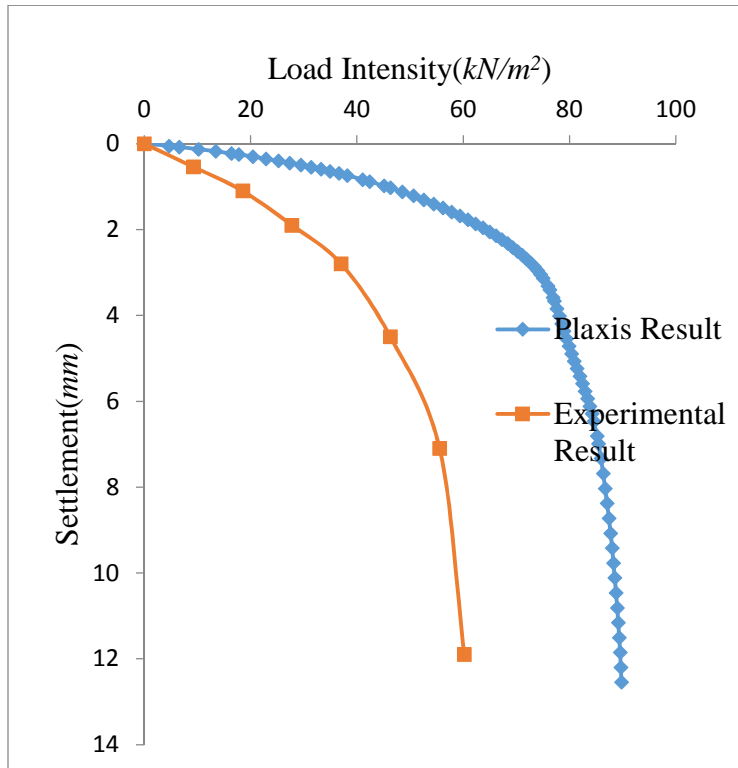


Figure 6.12: Comparison Load settlement curve at $D_f/B=0$, $e/B=0.15$

Table 6.2: Calculated value of q_u by PLAXIS 3D for eccentric condition along with experimental value

| e/B | D_f/B | Present Experiment; $q_u (kN/m^2)$ | PLAXIS 3D result; $q_u(kN/m^2)$ |
|-------|---------|------------------------------------------|---------------------------------------|
| 0 | 0 | 87 | 125 |
| 0.05 | 0 | 78 | 114 |
| 0.1 | 0 | 60 | 98 |
| 0.15 | 0 | 52 | 80 |
| 0 | 0.5 | 160 | 383 |
| 0.05 | 0.5 | 131 | 335 |
| 0.1 | 0.5 | 125 | 308 |
| 0.15 | 0.5 | 119 | 280 |
| 0 | 1 | 230 | 545 |
| 0.05 | 1 | 190 | 517 |
| 0.1 | 1 | 185 | 508 |
| 0.15 | 1 | 155 | 450 |

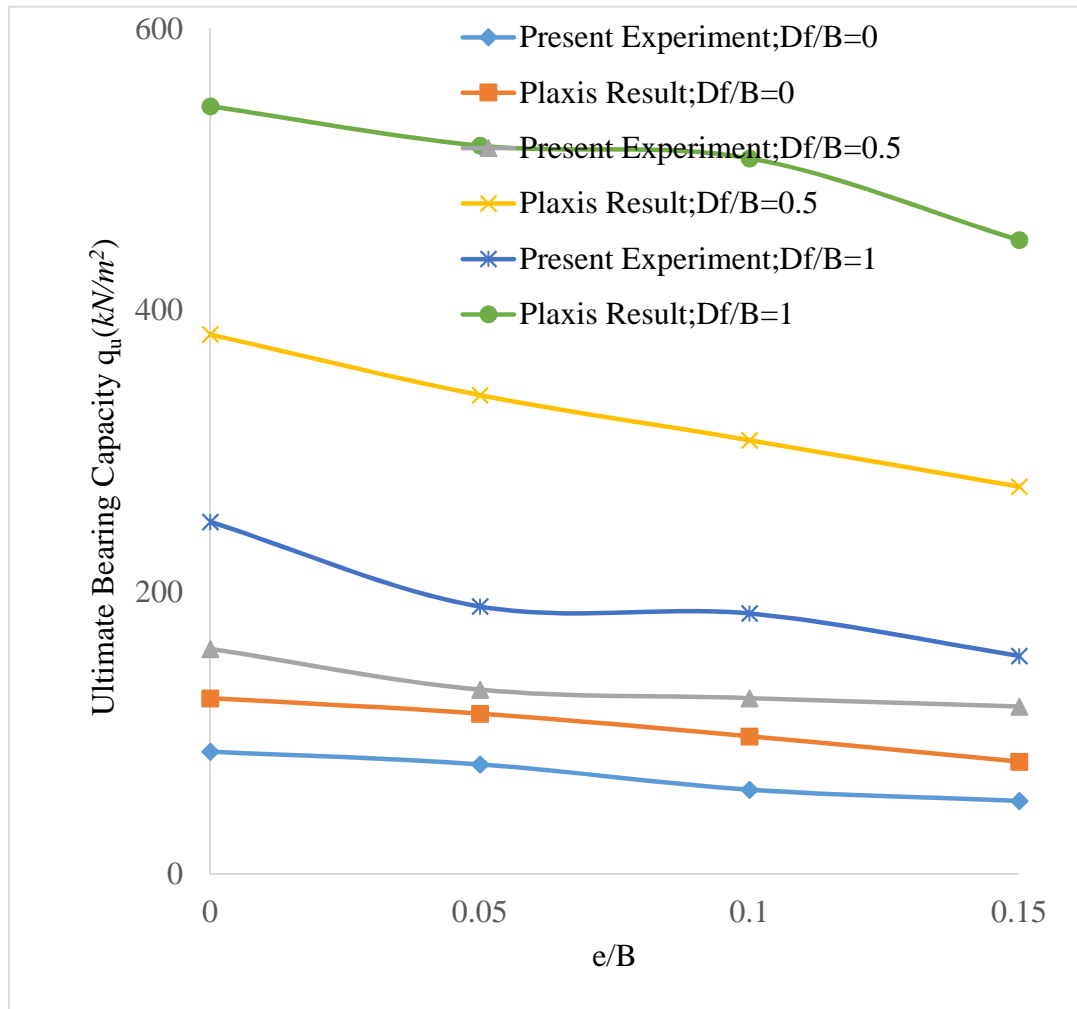


Figure 6.13: Comparison of ultimate Bearing capacity at different e/B (0, 0.05, 0.10, and 0.15) for present experiment results with PLAXIS 3D result

The nature of decrement of bearing capacity with the increase in eccentricity as observed from experimental results are with those using PLAXIS 3D results. It can be seen from Fig. 6.13 that the UBC by PLAXIS 3D method giving higher value than experimental UBC. UBC value increases by increasing the depth of embedment.

CHAPTER 7

CONCLUSION AND

SCOPE OF FUTURE

WORK

7.1 Conclusion

CONCLUSION AND SCOPE OF FUTURE WORK

As per numerical analysis following conclusions are drawn:

Numerical analysis and experimental analysis on model circular footing revealed that ultimate bearing capacity affected by depth of embedment (D_f/B), and different eccentric ratio e/B .

- Ultimate bearing capacity decreases by increasing the eccentricity (e/B) ratio for both surface and embedded condition.
- For the eccentric loaded circular footing, with increase in embedment depth bearing capacity increases.
- Maximum value of ultimate bearing capacity for each cases are obtained numerically in comparison to experimental.

7.2 Future research work

The present thesis is relevant to the study at different depth of embedment on the bearing capacity of eccentrically loaded circular footing on sand bed and eccentrically loaded at surface condition.

The future research work should address the below mentioned points:

- The present work can be extended to study the behavior of circular foundations of different sizes (Different diameter (B)) at different depth of embedment ($D_f/B=0.5, 1.0$)
- Large scale study should be carried out to validate the present developed equations. The present work can be extended to foundations on cohesive soil.
- The present work can be extended to reinforced soil condition for different depth of embedment.

- A generalized equation for Ultimate bearing capacity of reinforced sand bed can be derived for any shape (i.e. Circular, square, rectangular and strip) of footing.
- Present experiment have not been investigated for effect of other parameter (scale effect, different relative density, different type of soil etc.)

CHAPTER 8

REFERENCES

References

Basudhar,P.K.,Saha,Santanu.,Deb,Kousik (2007) “Circular footings resting on geotextile-reinforced sand bed” Department of Civil Engineering, IIT Kanpur Geotextiles and Geomembranes 25,pp.377–384.

Boushehrian,J.H.,Hataf,N., (2003) “Experimental and numerical investigation of the bearing capacity of model circular and ring footings on reinforced sand” Department of Civil Engineering, Shiraz University, Shiraz, Iran Geotextiles and Geomembranes 21(4),pp. 241–256.

Cerato A.B.,Lutenegger A.J., (2006) “Bearing capacity of square and circular footings on a finite layer of granular soil underlain by a rigid base” Journal of Geotechnical and Geoenvironmental Engineering ASCE vol.132,No.11,pp.1496-1501.

Dash,S.K.,Sireesh,S.,Sitharam,T.G., (2003) “Model studies on circular footing supported on geocell reinforced sand underlain by Soft clay” Department of Civil Engineering, Indian Institute of Science. Bangalore 560012. India Geotextiles and Geomembranes 21, pp.197-219.

DeBeer E.E., (1970) “Experimental determination of the shape factors and the bearing capacity factors of sand” Geotechnique 20, no.4: pp. 387-411.

Dewaikar,D.M.,Guptha,K.G.,Chore,S.H., (2011) “An Experimental Study into Behaviour of Circular Footing on Reinforced Soil "International scientific conference ,pp.630-634.

Elsaied,A.E.,Saleh,N.M.,Elmasha.M.E., (2014) “Behavior of circular footing resting on laterally confined granular reinforced soil” Construction Research Institute, Egypt, Civil Eng. Department, Benha University, Egypt, Housing and Building National Research Center,pp.1-6

Gupta, Ravi, Kumar, Rakesh, Jain, P.K., (2014) “behaviour of circular footing resting on three dimensional confined sand” International Journal of Advanced Engineering Technology Vol-V, pp.11-13.

Lovisa, J.,Shukla,S.K.,Sivakugan,N., (2010) “Behaviour of prestressed geotextile-reinforced sand bed supporting a loaded circular footing” Geotextiles and Geomembranes 28 ,pp. 23–32

Meyerhof G.G. (1953) “The Bearing Capacity of Foundations under Eccentric and Inclined Loads” In Proc. 3rd Int. Conf. Soil Mech. Zurich, vol. 1, pp. 440-45.

Meyerhof G. G. (1963). “Some recent research on the bearing capacity of foundation.” *Canadian Geotech. J.* 1(1), pp. 16-26.

Meyerhof G.G (1974). “Ultimate bearing capacity of footings on sand layer overlying clay” Can.Geotech j, 11, pp.223-229.

Nagaraj,T.K.,Ullgaddi,B.P., (2010) “Experimental Study on Load Settlement Behavior of Sand Foundations” Indian Geotechnical Conference GEOTrendz IGS Mumbai Chapter & IIT Bombay,pp.807-808.

Patra, C.R., Behera, R.N., Sivakugan, N., Das, B.M.(2012) “Ultimate bearing capacity of shallow strip foundation under eccentrically inclined load”: part I, International Journal of Geotechnical Engineering 6, no.3: pp. 343-352.

Patra, C.R., Behera, R.N., Sivakugan, N., Das, B.M. (2013) “Estimation of average settlement of shallow strip foundation on granular soil under eccentric loading” International Journal of Geotechnical Engineering 7,no.2, pp.218-222.

Prakash, S. and Saran, S. (1971) “Bearing capacity of eccentrically loaded footings”, *Journal Soil Mech. and Found Div.*, ASCE, 97: pp. 95–118.

Purkayastha, R.D., and Char, R.A.N. (1977) “Sensitivity analysis for eccentrically loaded footings.” *J.Geotech.Eng. Div.*, ASCE, 103(6), 647.

Rahman, M.G., (1981) “Bearing capacity and settlement of circular footing on sand “Department of civil Engineering Ottawa university Canada, pp.1-173.

Sitharam,T.G.,Sireesh,S., (2004) “Model studies of embedded circular footing on Geogrid-Reinforced sand beds” Department of Civil Engineering, Indian Institute of Science, Bangalore, India. *Ground improvement* 8, No. 2, pp. 69-75.

Sireesh, S., Sitharam, T.G. Dash, S.K., (2009) “Bearing capacity of circular footing on geocell–sand mattress overlying clay bed with void”. *Geotextiles and Geomembranes* 27, pp. 89–98.

Taiebat, H. A. & Carter, J.P. (2002) “Bearing capacity of strip and circular foundations on undrained Clay subjected to eccentric loads”. *Geotechnique* 52, no. 1, pp. 61–64.

Terzaghi, K. (1943) *Theoretical Soil Mechanics*, Wiley, New York.

Vesic, A.S., (1975) “Bearing capacity of Shallow foundations. In *Geotechnical Engineering Handbook*” Edited by Braja M. Das, Chapter 3, Journal Ross Publishing, Inc., U.S.A.